

Covalent Organic Frameworks (COFs): A New Class of Materials for Multivalent Metal-Ion Energy Storage Systems

Vedang A. Sonar,^[a] Abhishek A. Kulkarni,^[b] Prashant Sonar,^[b] and Deepak P. Dubal^{*[b]}

The rise of electronic societies is driving a surge in the demand for energy storage solutions, particularly in the realm of renewable energy technologies like batteries, which rely heavily on efficient electrode materials and separators. As an answer to this necessity, Covalent Organic Frameworks (COFs) are emerging and a highly intriguing class of materials, garnering increased attention in recent years for their extensive properties and possible applications. This review addresses the remarkable versatility and boundless potential of COFs in scientific fields, mainly focusing on multivalent metal ion batteries (MMIBs),

which include AIB (Aluminium-ion batteries), MIB (Magnesium-ion battery), CIB (Calcium-ion battery), and ZIB (Zinc-ion battery), as both electrode materials and separators across a spectrum of battery technology. Inclusive of their approaches, merits, and reaction mechanisms, this review offers an extensive summary of COFs concerning multivalent ion batteries. By providing a rigorous analysis of COF attributes, electrochemical behaviour, and methodologies, our explanation contributes to a deeper understanding of their potential in advancing battery technology.

1. Introduction

Over the preceding decade, scholars have increasingly shown interest in the domain of nanoporous materials due to their exceptional performance attributes and extensive utility across diverse applications. Notably, these applications encompass gas storage, gas separation, the engineering of superhydrophobic interfaces, energy conversion, optoelectronics, energy storage, water purification, and catalysis.^[1-3] During this temporal span, chemists have adeptly devised methodologies for synthesizing a wide range of porous materials, reflecting the vibrancy and progressiveness within the scientific landscape. In 2005, Yaghi and his colleagues unveiled a significant breakthrough by demonstrating the practicality of the topological design concept in synthesizing porous organic frameworks connected through covalent bonds. These pioneering frameworks represented the initial successful instances of covalent organic frameworks (COFs), making a crucial advancement in the field of materials chemistry.^[4,5]

COFs are a category of crystalline porous materials that are covalently bonded organic building blocks forming extended structures and the backbone of these structures consists of lightweight elements.^[6] One notable benefit of covalent connectivity lies in its ability to confer robustness to COFs, thereby establishing a versatile framework for customizable materials design. Researchers have been able to anticipate the structure of resultant COFs with a notable degree of accuracy because the organic components of COFs retain their overall geometry

upon linkage. This characteristic has facilitated the intentional synthesis of COF structures and enabled their creation with specific composition as well as specific pore sizes and apertures.^[7,8] Since advantageous properties of COFs result from complex interactions of organic material properties such as electron delocalization, the rigidity of the structure, flexibility, and polarity, there is a great deal of diversity in the types of COFs used in different applications such as porous, conjugated, functionalized and hybrid COFs.^[9] Within the domain of COFs, 3D structures as well as 2D layered structures are synthesized based on the geometry and the connectivity of organic building units.^[10] 2D COFs created through the layering of organic materials offer diverse pore sizes and high surface areas, making them perfect for gas storage applications. Optimal 2D COFs featuring π -conjugated systems and short distances between layers, hold promise for electronic interactions among the sheets, potentially leading to conductivity.^[11]

COFs have emerged as fascinating material that gained substantial interest due to their distinctive characteristics, positioning them as outstanding candidates for diverse applications within scientific domains.^[12] The versatile aspects of the COFs are attributed to their diverse molecular engineering opportunities to tune their properties based on the nature of the application. The COFs create porosity which can be used for gas separation, gas storage, water purification, energy storage (electrode material for cation shuttle and separator for battery), guest-host sites for chemical interaction, bio(chemical) sensing, pore channels for ion transport and many more.^[13] In recent times, the catalytic activity of metals was specifically underscored via the catalytic coordinating entities, available in COF structures. Furthermore, their application extends to serving as organocatalysts, thereby contributing to the border landscape of catalytic processes.^[14] In addition to this, conjugated COF can be used as an active channel semiconductor in organic field effect transistors (OFETs), energy harvesting layer in organic solar cells (OSC), and emitting layer in organic light-emitting

[a] V. A. Sonar

Department of Chemistry, School of Advanced Sciences, Vellore Institute of Technology, Vellore -632014, India

[b] A. A. Kulkarni, P. Sonar, D. P. Dubal

Centre for Material Science, Department of Chemistry and Physics, Queensland University of Technology, Brisbane, QLD 4000, Australia

E-mail: dubaldeepak2@gmail.com

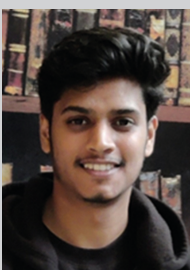
deepak.dubal@qut.edu.au

diodes (OLEDs). It also has the potential to be them for drug delivery applications due to tuneable porosity. Among various diverse applications, particularly COF applications in gas storage are remarkable since they consist of low-density lightweight elements, exhibiting a notable potential for enhanced gravimetric storage capacity. This makes it highly promising in gas storage, capitalizing on its composition to achieve improved storage capabilities.^[14–17]

In energy conversion and energy storage technologies, the increasing need for top-notch energy storage solutions has provoked remarkable progress. More reliable and efficient secondary batteries, particularly lithium-ion batteries (LIBs) have secured tremendous consideration in recent times due to their applications in various fields including mobile phones, personal tablets, and electrical vehicles (EVs). Due to the LIB innovation, traditional fossil fuel energy sources will be replaced globally.^[18–20] The evolution of electronics and electric vehicles (EVs) necessitates enhancements in battery performance metrics, including capacity, charging rate, and safety. Central to this endeavor is the exploration of superior electrode and electrolyte materials. Porous materials emerge as auspicious candidates for advancing energy storage and conversion technologies on account of their ordered porous structure, which facilitates rapid ionic transport and storage while minimizing volume fluctuations.^[16] The structural versatility and molecular level tunability of these materials holds promise for unravelling

the underlying mechanism governing battery options.^[21–24] Due to the favourable characteristics exhibited by COFs, significant strides have been made in their utilization within battery systems. COFs have been exploited not only as electrodes but also as separators in various types of batteries, involving LIBs,^[25] SIBs (Sodium-ion batteries),^[26] KIBs (potassium ion batteries),^[27] CIBs,^[28] Na–S (Sodium Sulphur) batteries, etc. (Figure 1) underscoring their considerable promise in advancing battery.

Recent publications on COFs for MMIBs have primarily focused on synthesizing potential COF materials, strategies for improving electrochemical performances, and advancements in electrode materials.^[23,29–34] This review not only explores the properties and applications of COFs in MMIBs but also delves into the mechanisms by which COFs function as anode and cathode materials, as well as their role as electrolytes and separators. This review provides a detailed summary of the latest advancements in electrode materials and separators, covering a range of battery types including ZIB, MIB, CIB, and AIB. Additionally, it addresses the current challenges and offers insights into the future directions for enhancing COF-based electrodes, separators, and electrochemical performances as well. We believe this review will serve as a valuable guide for researchers, paving the way for future innovations in the use of COFs in battery technology.



Vedang Sonar recently completed his M.Sc. in General Chemistry from Vellore Institute of Technology (VIT), India. His research interests include covalent organic frameworks (COFs) and multivalent ion batteries, with experience in polymer synthesis and energy storage materials.



Abhishek Kulkarni is pursuing his doctoral studies at Queensland University of Technology (QUT) with Prof. Deepak Dubal. His academic journey commenced with the attainment of an integrated B. Sc – M. Sc. Degree in Nanoscience and Technology from Shivaji University Kolhapur, India, before joining QUT. His research concentrates on the development of non-metal ion-based energy storage systems and sustainable energy solutions.



Prashant Sonar performed doctoral research under Prof. K. Mullen at the Max-Planck Institute for Polymer Research and was awarded a Ph.D. in 2004. He worked as a Postdoctoral Fellow at ETH Zurich (Switzerland) and a Research Scientist at A*STAR (Singapore). He is currently a Professor at Queensland University of Technology, Australia. He is a recipient of the prestigious ARC Future Fellowship, a Fellow of the Royal Chemical Society and Maharashtra Academy of Science, and also serves as an associate editor for Flexible and Printed Electronics. His research activities are focused on organic electronics, material synthesis, and optoelectronic devices.



Dr. Deepak P. Dubal is a Professor at the Queensland University of Technology (QUT), Australia, known for his outstanding contributions to the field of supercapacitors, batteries and triboelectric/piezoelectric nanogenerators. He has earned multiple prestigious fellowships throughout his career, including the Brain Korea-21 (South Korea-2011), Alexander von Humboldt (Germany-2012), Marie Curie (Spain-2014), Vice-Chancellor Fellowship (Australia-2017) and ARC – Future Fellowship (Australia-2018). He receives regular international recognition for his work including being listed one of Australia's top-100 Materials Scientists and elected as Foreign Young Associate Fellow of Maharashtra Academy of Sciences (FFMAS), India.

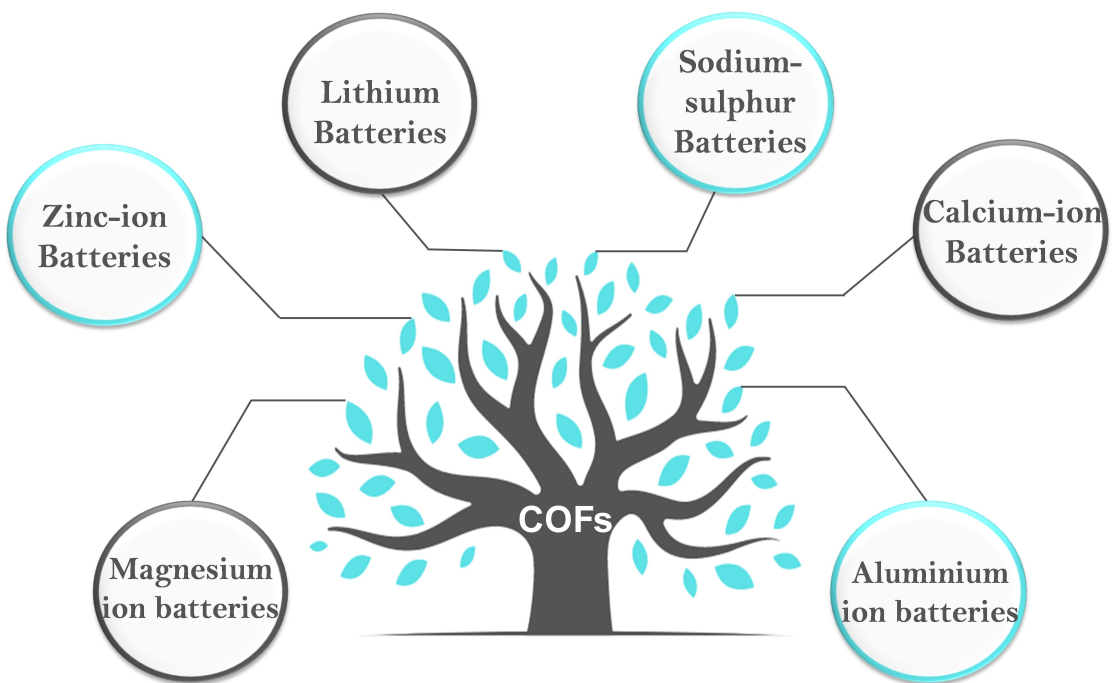


Figure 1. Applications of COFs in various batteries.

2. Working Mechanism of COFs in Battery

In the realm of electrochemical energy storage, rechargeable batteries serve as vital devices that can convert electrical energy into chemical energy, storing it within the battery's chemical components during charging, and subsequently releasing this stored energy as electrical output during discharge.^[35,36] It is typically composed of essential components such as an anode, cathode, electrolyte, and separator, and these batteries facilitate the transfer of charge through the movement of ions between two electrodes. An electrolyte-filled separator enables ion transport during charging/discharging and prevents direct electrode contact.^[37] The efficiency of charge transfer hinges upon the interaction between the active ion and the electrode material, with various mechanisms dictating this process. The charge storage capacity of the battery correlates with the potential difference between electrochemical reactions occurring at the electrodes and the number of electrons involved in each reaction. To achieve cost-effective battery cells, battery engineers employ two main strategies: material selection and morphology optimization. Utilizing economically viable, readily available materials that can be tailored into appropriate physical forms is essential in realizing low-cost battery technologies.^[38]

The working mechanism of COFs in rechargeable batteries depends upon the charge states of organic components within the COFs when the change occurs reversibly during the operation of the electrode. Organic molecules or groups within COFs can accept or release ions in a controlled and reversible manner as the battery undergoes the charging and discharging cycles. Organic electrode materials are placed under two categories based on the charge state they attain during redox reactions: n-type and p-type.^[39] i) N-type organics: They are

lessered to form negatively charged anions throughout the reduction reaction process. Taking the example of LIB, with the decrease in COFs there will be an equilibrium of negatively charged species with the help of cations moment (Li^+), completing a charge/discharge process. ii) P-type organics: They are oxidized to form positively charged cations during the reaction process.^[40,41] Electrode materials derived from COFs are capable of being conceptualized as redox-active sites encapsulated inside a porous organic framework. Consequently, integrating redox units towards the framework represents a direct approach to fabricating COF electrode materials.

3. Synthesis Methods of COFs

COFs are designed using a topology approach, where the geometry of building blocks directs the formation of polygonal skeletons. These polygons, made of knot and linker units, vary in shape and size based on the geometries of the monomers as starting materials, influencing pore dimensions based on organic framework established while connecting monomers. Commonly observed COF structures include hexagonal, rhombic, tetragonal, kagome, and trigonal type geometries and these are governed by functionality and geometries of monomers. For example, the formation of hexagonal COFs can arise from C_2 -symmetric or C_3 -symmetric units. In 2D COFs, layers are connected through $\pi-\pi$ interactions and intralayer covalent bonds, while 3D COFs require Td or orthogonal symmetry in knot units to grow the polymer network in three dimensions. Additionally, specific topology combinations like $[Td + C_3]$ for **ctn** and **bor**^[42] networks, and $[Td + C_2]$ or $[Td + Td]$ for **dia**^[43] networks, prevent interpretation, and enable high surface areas.

The **dia** network forms the largest family of 3D COFs due to its compatibility with a wide range of C_2 -symmetric linkers. The symmetry-driven design forms the core principle behind the structural diversity of COFs.^[44–46] In Figure 2, some common topology diagrams of 2D and 3D COFs are given.

This section outlines various synthesis techniques employed in COF preparation, including solvothermal, ionothermal, microwave-assisted, and mechanochemical methods. Solvothermal synthesis is one of the most commonly used approaches, where monomers react in a solvent under elevated temperature and pressure to yield highly crystalline frameworks. In contrast, in ionothermal synthesis, ionic liquids get utilised as both solvents and catalysts while preparing MOFs. Microwave-assisted synthesis provides rapid reaction within shorter times by applying microwave radiation to accelerate the formation of COFs. Lastly, mechanochemical method involves solid-state reactions driven by mechanical forces, eliminating the need for solvents.

3.1. Solvothermal Synthesis

Among all the investigated synthesis methods, the solvothermal method is one of the most popular methods for synthesizing COFs till date. The reaction conditions in this approach are largely influenced by the reactivity and solubility of the building blocks, as well as the reversibility exhibited by the reactions. A mixture of suitable monomers for the edges and vertices, along with a catalyst and a solvent or solvent mixture, is placed in a closed reaction vessel such as a Pyrex tube, steel autoclave with

a Teflon liner, or a glass container with a sealed cap while employing the solvothermal method.^[47] During conducting solvothermal reaction, the reaction mixture is sonicated briefly, degassed using freeze-pump-thaw cycles, and the vessel is enclosed. The reaction is carried out at a temperature exceeding the solvent's boiling point, which enhances precursor solubility and reaction kinetics. After the reaction time has elapsed, the system is cooled down to a room temperature for thermal stabilization. The solid product is then recovered through centrifugation or filtration and further washed with a suitable solvent or subjected to Soxhlet extraction for removing oligomers or exchanging high-boiling-point solvents.^[48,49]

The solvothermal synthesis of COFs utilizes thermal energy to shift the reaction equilibrium toward the formation of thermodynamically stable crystalline structures, which typically require prolonged reaction times and significant energy input. To address this limitation, alternative energy sources have been explored to accelerate the nucleation process of crystallites and to synthesize COFs more efficiently, thereby increasing the overall synthesis rate of COFs.^[14]

3.2. Ionothermal Synthesis

Ionic liquids, which are organic salts composed entirely of cations and anions, exist in a liquid form at or near room temperature and are often referred to as low-temperature molten salts. Due to their distinct properties, such as high stability, low volatility, and environment friendliness, ionic

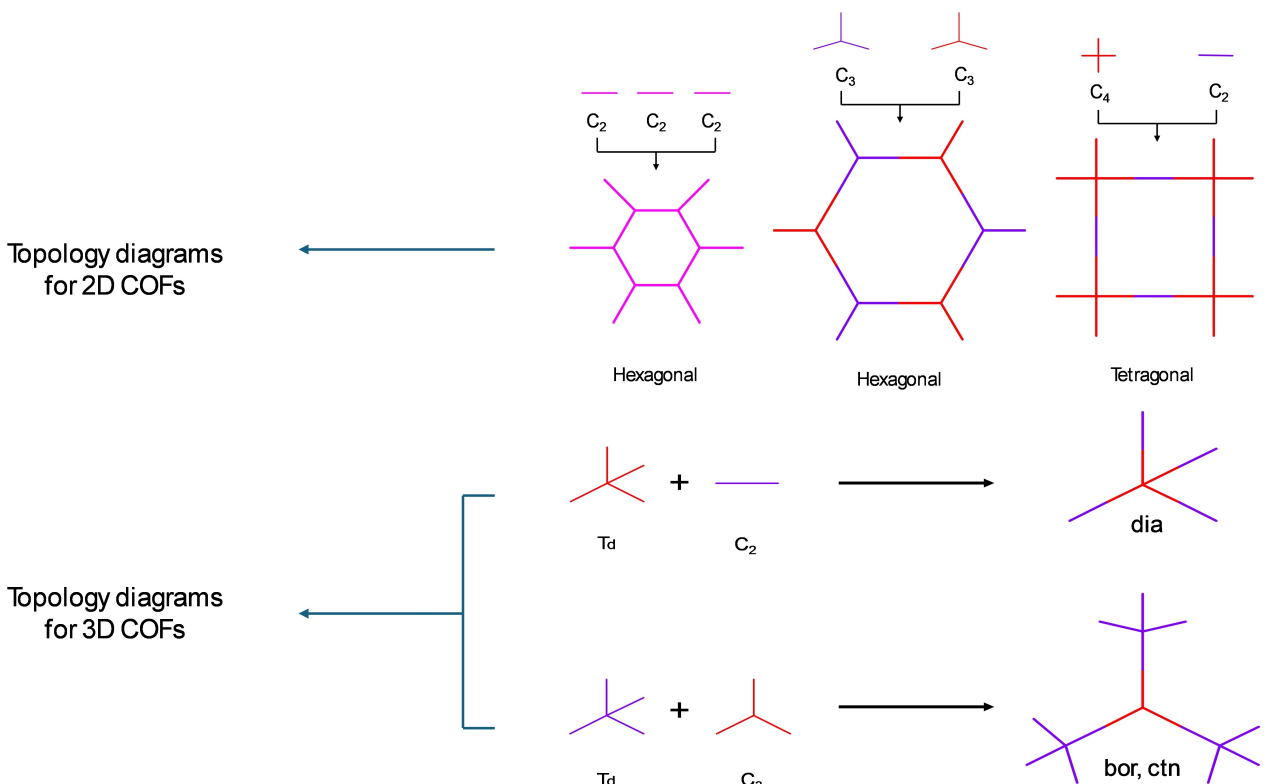


Figure 2. Some common 2D and 3D COF topology diagrams.

liquids are considered as a green and safe solvents. They have been extensively and widely used as recyclable reaction media in organic synthesis.^[50]

In ionothermal methods, ionic liquids or molten salts serve as solvents as well as catalysts, with reactions typically conducted at elevated temperatures. Although generally used monomers in this method are amorphous and lack long-range molecular ordering, the use of ionic liquids in COF synthesis offers a simple, mild, and environmentally friendly approach. Bojdys and colleagues prepared the first COF using the ionothermal method.^[51] Compared to the solvothermal method, ionothermal synthesis does not rely on the solubility of the precursors, and the reaction time is significantly reduced, making it a more efficient and versatile approach.

3.3. Microwave Synthesis

Microwave synthesis has gained significant attention because of its distinct advantages, including faster reaction rates, higher product yields, and reduced energy consumption. Unlike solvothermal methods, which require extended reaction times, microwave synthesis has been investigated for the expeditious production of crystalline COFs. In a typical microwave synthesis, monomers are dissolved in an appropriate solvent and the mixture is enclosed in a microwave tube under a vacuum or nitrogen, then heated while stirring at a set temperature, such as 100 °C, for 60 minutes followed by an additional 10–20 minutes for solvent extraction. The formed precipitate is isolated through filtration and then drying under a vacuum environment. This approach is particularly effective at removing oligomers, leading COFs with enhanced porosity. Compared to ionothermal and solvothermal synthetic methods, microwave synthesis offers significantly shorter reaction times and produces cleaner and pure products, making it an efficient and environmentally favourable method.^[52]

3.4. Mechanochemical Synthesis

Mechanochemical synthesis has gained prominence as an effective and environmentally friendly approach synthesis of functional materials via green approach due to its simplicity, cost-effectiveness, and eco-friendly nature. It has become one of the advanced methods for preparing COFs. This technique which operates at room temperature without the need for solvents, is as straightforward and starting materials or precursors needs to be grinded.^[53] The advantages of mechanochemical synthesis include mild reaction conditions, straightforward operation, and a low environmental impact, making it a widely used method for producing porous organic materials. COFs produced via this solvent-free approach exhibit good thermal stability and high chemical resistance in harsh environments, such as acidic, basic, or boiling water conditions. However, these COFs typically have moderate crystallinity and lower BET surface areas compared to those synthesized through the solvothermal method. In addition, both microwave and

mechanochemical synthesis techniques offer the benefits of short reaction times, high product yields, and potential scalability, positioning them as key methods for the future.^[54,55]

4. Structure-Performance Relationship of COFs

In multivalent ion batteries, micro, molecular, and electrode structures of COF electrode materials largely affect the electrochemical performance. The theoretical capacity is determined by the number of redox-active sites available per molecular weight, while practical capacities depend on factors such as particle size, conductivity, and pore size. These structures tuned via molecular engineering affect electron and ion transfer, impacting the rate performance. Modifying both the linking groups and building blocks is an effective approach to optimize the number of active sites available, which enhances the overall capacity of electrode materials. Additionally, molecular structure plays a crucial role, with p-type redox linkages generally yielding higher voltages than n-type. The inclusion of electron-withdrawing or donating groups can modify the LUMO energy level, affecting voltage and capacity of the battery. COFs with optimal pore size and high conductivity are more likely to approach their theoretical capacity, but factors like linkage stability and redox activity can limit cycling performance. Understanding the relationship between structure and performance is key to optimizing COFs for practical applications in various multivalent ion batteries.^[56–59]

5. COFs as Additives and Electrolytes

Not only COFs are getting attention for a wide range of applications but also their potential use as both additives and electrolytes in energy storage systems. The presence of well-ordered 1D (one-dimensional) channels, coupled with their robust stability against phase transitions, makes COFs a promising and ideal candidate for solid electrolytes.^[60] Compared to inorganic ion conductor counterpart, COFs offer several key advantages due to their permanent porosity, structural tunability, and enhanced chemical stability. Inorganic conductors are typically more brittle, chemically harder to modify, and unstable in air, which limits flexibility in applications requiring mechanical robustness and long-term reliability. Moreover, COFs can be classified as either neutral or ionic based on their charge characteristics.^[61] Ionic COFs, in particular, exhibit permanent open channels and tunable pores composed of charged building blocks, which enable extensive ion-ion and ion-dipole interactions. These properties are especially attractive for energy storage systems, where ionic COFs could be employed as solid-state electrolytes, modification layers for separators and electrodes, or additives in electrode materials.^[62,63]

The use of COFs as additives has seen significant interest, especially in improving electrode performance. For instance, Tang et al.^[64] demonstrated that incorporating a small amount of electropositive COFs into polymer cathodes substantially

enhanced their intercalation kinetics of large-size anions. This modification resulted in remarkable improvements in the capacity, rate performance, and cyclability of the batteries. The ability of COFs to enhance ion transport and stabilize electrode interfaces makes them highly promising for next-generation battery technology.

6. COFs in Multivalent Metal Ion Batteries (MMIBs)

Rechargeable MMIBs encompass MIB, ZIB, AlB, and CIB. Owing to their advantageous properties like abundant resources, high electron redox capability, and low reactivity in atmospheric conditions, MMIBs are being explored as viable alternatives to LIBs.^[29] The performance characteristics of MMIBs including cycle stability, power density (PD), and energy density (ED), are significantly influenced by electrode materials, thereby driving extensive investigations in this area is critical for the development of next-generation energy storage systems.^[29,80,81]

COFs are recognized as prospective electrode materials owing to their distinctive attributes, encompassing inherent insolubility in electrolytes, ample porosity, precise open channels facilitating ion migration, and π -conjugated extended framework enhancing charge transfer.^[39,82,83] Diverging from conventional organic electrode materials, COFs exhibit resilient frameworks characterized by crystalline structures and high porosity opening a new gate for innovative material designs. Table 1 summarizes different COFs along with their

applications, electrolytes, voltage windows, capacity, capacity retention, and number of cycles.

6.1. Role of COFs as Cathode Material in Zinc-Ion Batteries

In the realm of energy storage materials, ZIBs are being deemed as the new potential alternatives for widely used LIBs. Since it is abundant, environmentally friendly, cost-effective, and safer in comparison to LIBs, it has gained a lot of interest from researchers worldwide.^[84–87] However, the commercialization of ZIBs is difficult as of now since it demands high ED. Elevating the operational voltage is a good strategy for ZIBs but it necessitates pronounced voltage cathode materials against Zn^{2+}/Zn . Recent advancements focus on enhancing ZIB batteries' long-term cyclability, ED, and stability using potential cathode materials.

Zheng and colleagues^[68] introduced a novel COF based on orthoquinone for ZIBs as a cathode material. The synthesis procedure was guided by the structural design and ordered channel arrangement, employing benzenetricarboxaldehyde (BT) and pyrene-4,5,9,10-tetraone (PTO) through a Schiff-based solvothermal condensation reaction to yield BT-PTO-COF (Figure 3a). The cyclic voltammetry (CV) in Figure 3b, indicated three peaks for reduction and two peaks for oxidation during the analysis of BT-PTO-COF, and these peaks align with three distinct redox states of COF while cation de-insertion and insertion. The electrochemical investigations of BT-PTO-COF primarily focused on utilizing 3 M $Zn(CF_3SO_3)_2$ electrolytes due to their enhanced wettability and ion conductivity properties. BT-PTO-COF exhibits 225 mAh g^{-1} of an outstanding reversible

Table 1. Summarized Application of COFs in various batteries. (ZIBs, CIBs, MIBs and AlBs).

COFs	Applications	Electrolyte	Potential window (V)	Capacity (mAh g^{-1} at Ag^{-1})	Capacity retention (%)	Number of cycles	Ref.
PI-COF	Anode	2 M $ZnSO_4$	−0.9–0	92 at 0.7	85	4000	[65]
Tp-PTO-COF	Cathode	2 M $ZnSO_4$	0.4–1.5	218.5 at 2	95	1000	[66]
COF-PTO	Cathode	1 M $Zn(CF_3SO_3)_2$	0.2–1.6	105 at 10	98	18000	[67]
BT-PTO COF	Cathode	3 M $Zn(CF_3SO_3)_2$	0.4–1.6	221 at 1	98	10000	[68]
COF-TMT-BT	Cathode	2 M $Zn(CF_3SO_3)_2$	0.5–1.6	283.5 at 0.1	96.2	2000	[69]
TA-PTO-COF	Cathode	2 M $ZnSO_4$	0.6–1.4	255 at 0.1	–	1000	[70]
TfDa-COF	Cathode	2 M $ZnSO_4$	0–1.6	96.6 at 0.1	98	10000	[71]
PTHAT-COF	Anode	6.67 M $CaCl_2$	−0.6–−1.05	106.6 at 0.25	89.9	10000	[72]
HqTp-COF	Cathode	1 M $CaCl_2$	0–1.7	119.5 at 1	73.7	1600	[73]
TB-COF	Anode	3.4 M $CaCl_2$	0–1.9	253 at 1	74	3000	[74]
Trizine based COF	Cathode	0.5 M $Mg(TFSI)_2$	0.8–2.5	107 at 0.02	99.4	3000	[75]
HAQ-COF	Anode	1 M $MgSO_4$	0–1.5	105.8 at 1	85.6	10000	[76]
DATP-CNT@20 COF	Cathode	$AlCl_3/EMIC$	0–2.5	140 at 1	100	2400	[77]
DAQ-TpO COF	Cathode	$AlCl_3/EMIC$	0.3–2.2	290 at 0.2	92.5	32000	[78]
TpBpy-COF	Cathode	$AlCl_3/[EMIm]Cl = 1.3$	0.01–2.3	150 at 2	–	13000	[79]

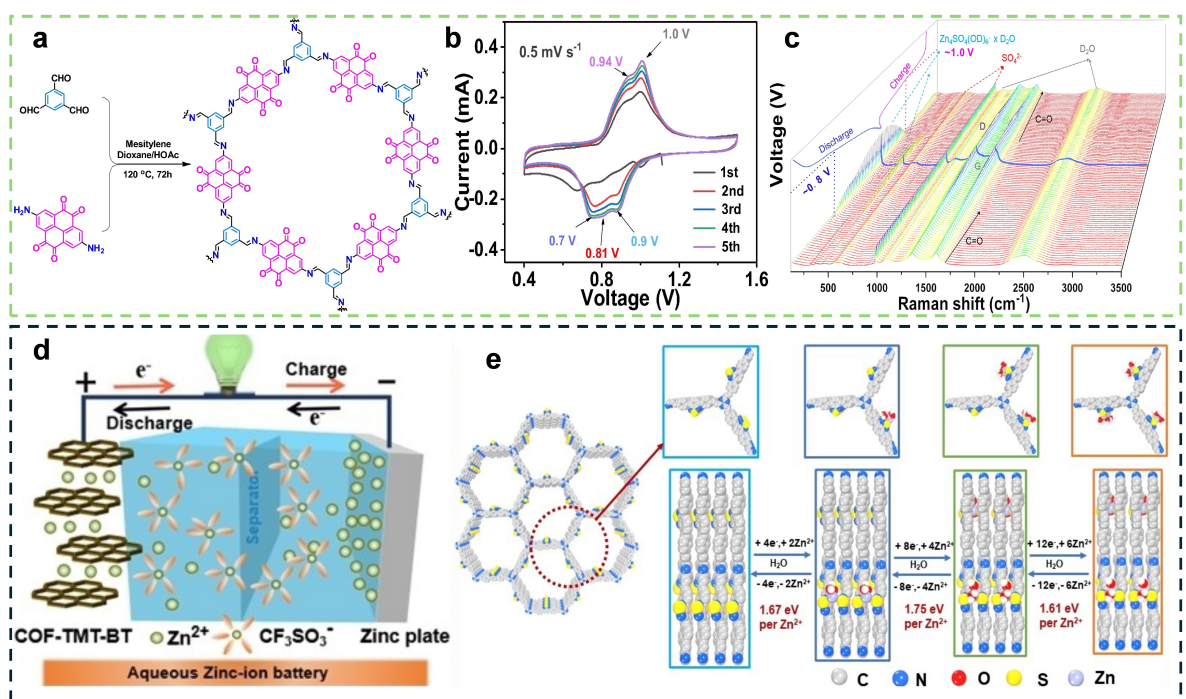


Figure 3. (a) The synthetic pathway for BT-PTO-COF. (b) CV profile employing a SR of 5 mV s^{-1} . (c) BT-PTO-COF *in situ* Raman spectrum in electrolyte 3 M ZnSO_4 . Reproduced with permission from ref.^[68] 2022 Wiley. (d) Representation of zinc battery using COF-TMT-BT. (e) Binding energy representation for COF-TMT-BT at each stage of zirconation. Reprinted with permission from ref.^[69] Copyright 2023 Wiley.

capacity at 0.1 A g^{-1} and impressive long-term cyclability, with a retention rate of 98.0% at 5 A g^{-1} after 10,000 cycles. After doing the kinetic analysis, they found for the first time that it validates the presence of a redox pseudocapacitive mechanism, characterized by the initial insertion of Zn^{2+} ions followed by the subsequent co-insertion of two H^+ ions. To confirm this mechanism *in-situ* Raman analysis (Figure 3c) was conducted which displayed regular fluctuations of peaks at 166 and 436 cm^{-1} along with other subtle peaks, altogether serving as direct evidence for H^+ insertion.^[88,89] Notably, this co-insertion manner transitions to predominantly H^+ insertion paths at higher current densities (CDs), resulting in ultra-fast kinetics and 184 kW kg^{-1} (COF) of an unprecedented specific power alongside 92.4 Wh kg^{-1} (COF) of a high ED.

Peng et al.^[69] reported a new structurally stable olefin-linked COF-TMT-BT, which was composed through Brønsted acid-catalysed aldol condensation between 2,4,6-trimethyl-1,3,5-triazine (TMT) and also the 4,4'-(benzothiadiazole-4,7-diy) dibenzaldehyde (BT). This synthesis strategy incorporates benzothiadiazole units as innovative electrochemically active moieties within the framework. COF-TMT-BT material includes non-reversible C=C linkages, rendering it unable to dissolve in the aqueous-based electrolytes, featuring benzothiadiazoles as electrochemically active units within the structure. They prepared an aqueous ZIB using $\text{Zn}(\text{CF}_3\text{SO}_3)_2$ as the electrolyte, COF-TMT-BT as the cathode, and Zn foil as the anode materials respectively (Figure 3d).

Nitrogen and sulphur have higher electronegativities than carbon, and their incorporation in benzothiadiazole units

within COF-TMT-BT not only improves electrochemical activity and performance but also enables tailored ion coordination mechanisms. COF-TMT-BT binding energy (BE) was calculated following the redox reaction with Zn^{2+} by using model compounds (Figure 3e). Notably, after Zn^{2+} uptake the $\text{Zn}_6@\text{COF-TMT-BT}$ model exhibited stable configuration among all others. COF-TMT-BT demonstrated great potential and promising characteristics as a cathode material for ZIB, displaying a 283.5 mAh g^{-1} specific capacity (SC) at 0.1 A g^{-1} alongside 219.6 Wh kg^{-1} of an exceptional ED and 23.2 kW kg^{-1} of power densities, and the electrodes retain a SC value of 186.8 mAh g^{-1} over 2000 cycles. These performance metrics surpass most of the COF-reported cathodes known to date.

An exciting new direction for the study of self-charging ZIBs has been going on, but currently, there is no universally accepted protocol for examining the self-charging capabilities of cathode materials. Cathode materials are crucial for the self-charging functionality of ZIBs since their charging process is obtained through the redox reaction between O_2 and cathode. Zhong et al.^[67] successfully synthesized a COF with pyrene-4,5,9,10-tetraone groups named COF-PTO and mentioned it ZIBs' upcoming cathode materials. They also proposed a method for the assessment of its self-charging performance based on two factors, i.e., the self-charging efficiency (η) and the average self-charging rate (v). An outstanding η of 96.9% was achieved by COF-PTO and 30 mAh g^{-1} throughout 100 self-charging cycles. It also showed an exceptional capacity retention (CR) of approximately 98% for 18,000 cycles at 10 A g^{-1} . They did the mechanisms study and found out that

COF-PTO has abundant carbonyl groups, which enable the co-insertion of double ions (Zn^{2+} and H^+) to obtain self-charging performance. One of the most important things researchers discovered is that the COF-PTO electrode demonstrates notable η because of the generation of metal heterocyclic complexes among COF-PTO and Zn ions, which promotes the self-charging reaction. Researchers also developed a proficient self-charging mechanism which can be seen in Figures 4a and 4b, comprising three key steps: (a) Co-insertion of Zn^{2+} and H^+ into electrolyte $Zn(OTf)_2$ leading to a complete phase of discharge. (b) Gradual release of H^+ and Zn^{2+} in the presence of oxygen generates TP-PTO, facilitating self-charging (Figure 4a- step 1). (c) Spontaneous generation of metal heterocyclic complexes with carbonyl and $-NH-$ occurs (Figure 4a-step 2), resulting in a decrease in TP-PTO production. This leads to an accelerated rate of TP-PTO formation from 3H-TP-PTO-Zn₂H, akin to Le Chatelier's principle.^[69]

The redox-active components in the COFs are capable of being controlled at the molecular scale, yielding a substantial capacity, but given that most COF electrodes consist of only one active redox moiety, this naturally leads to reduced theoretical and functional capability. Hongbao Li et al.^[70] documented the successful design and fabrication of a COF material consisting of dual redox sites (C=O and C=N), named TA-PTO-COF. The synthesis of TA-PTO-COF (Figure 5a) was done by a Schiff-based reaction between 2,7-diaminopyrene-4,5,9,10-tetraone (PTO-NH₂) and tris(4-formylbiphenyl)amine (TA). Several electrolytes were used for the testing of the TA-PTO-COF cathode, but 2 M $ZnSO_4$ displayed more cycling stability and competitive capacity.

TA-PTO-COF has been observed as a potential candidate for cathode material since it shows great results when compared with the PTO-NH₂ monomer, like high discharge capacity (255 $mA\cdot h g^{-1}$), outstanding performance of rate (186 $mA\cdot h g^{-1}$ at 10 $A g^{-1}$), along with long-period cyclability which is 1000 cycles at 1 $A g^{-1}$, and 84% high initial coulombic efficiency (ICE). Despite the fact that undergoing 100 cycles, the material demonstrates the ability to sustain 176 $mA\cdot h g^{-1}$ of reversible capacity. In contrast, utilization of the PTO-NH₂ monomer resulted in only 131 $mA\cdot h g^{-1}$ of retention. Figure 5b illustrates the rate capability of both PTO-NH₂ monomer and TA-PTO-COF across distinct CDs (ranging from 0.1–10 $A g^{-1}$). The voltage recorded for the pouch cell stands at 1.193 V. Furthermore, the pouch cell demonstrates effective operation, evidenced by the illumination of LED lamps, even when subjected to folding, thereby showing the commendable grade of safety associated with the pouch cell's performance (Figure 5c–e). On performing characterizations like ex-situ Fourier-transform infrared spectroscopy (FTIR) and X-ray photoelectron spectroscopy (XPS), researchers found out that the C=O and C=N bonds within TA-PTO-COF exhibit reversible cation acceptance and release from the electrolyte.

Lastly, Lihua Li et al.^[71] synthesized two COFs, namely, TfDa-COF which is a COF based on anthraquinone, and TpDa-COF which is a COF based on anthracene. Both the COFs TfDa-COF and TpDa-COF were fabricated using a solvothermal condensation reaction involving 1,3,5-triformylphloroglucinol (TFP) with 2,6-diamino anthraquinone (DAAQ) and separately with 2,6-diamino anthracene (DA). The contribution of the keto-enol tautomerism C=O groups in TfDa-COF to the battery capacity is merely 4.8% when compared to TpDa-COF. The

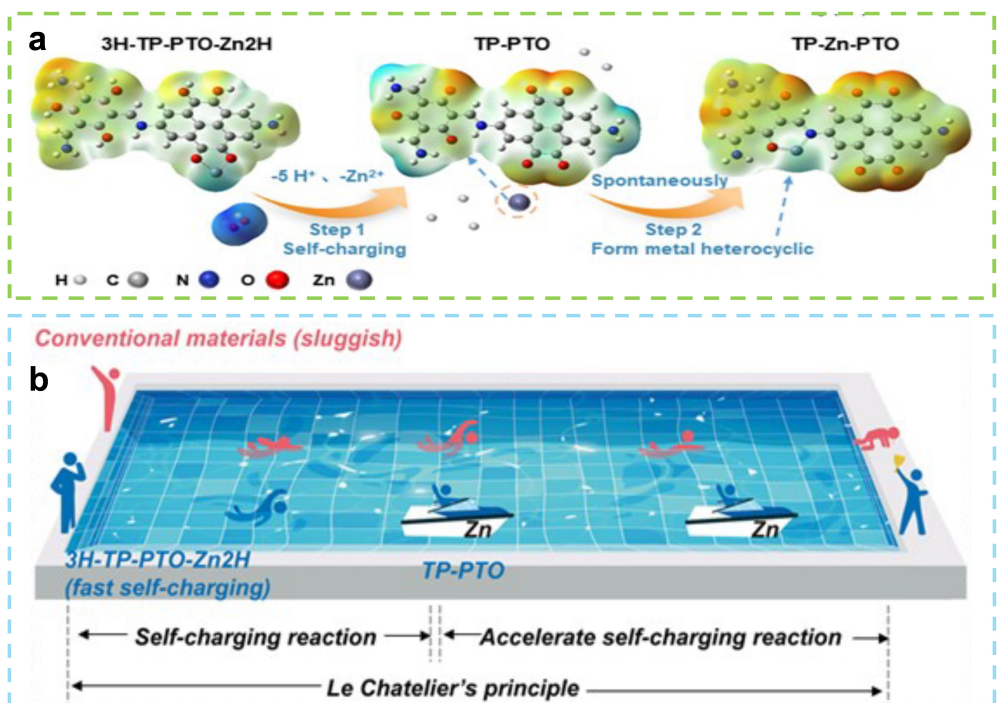


Figure 4. (a) Diagram illustrating Le Chatelier's principle to facilitate self-charging reactions. (b) Schematic representation elucidating the self-charging mechanism. Reprinted with permission from ref.^[67] Copyright 2024 Wiley.

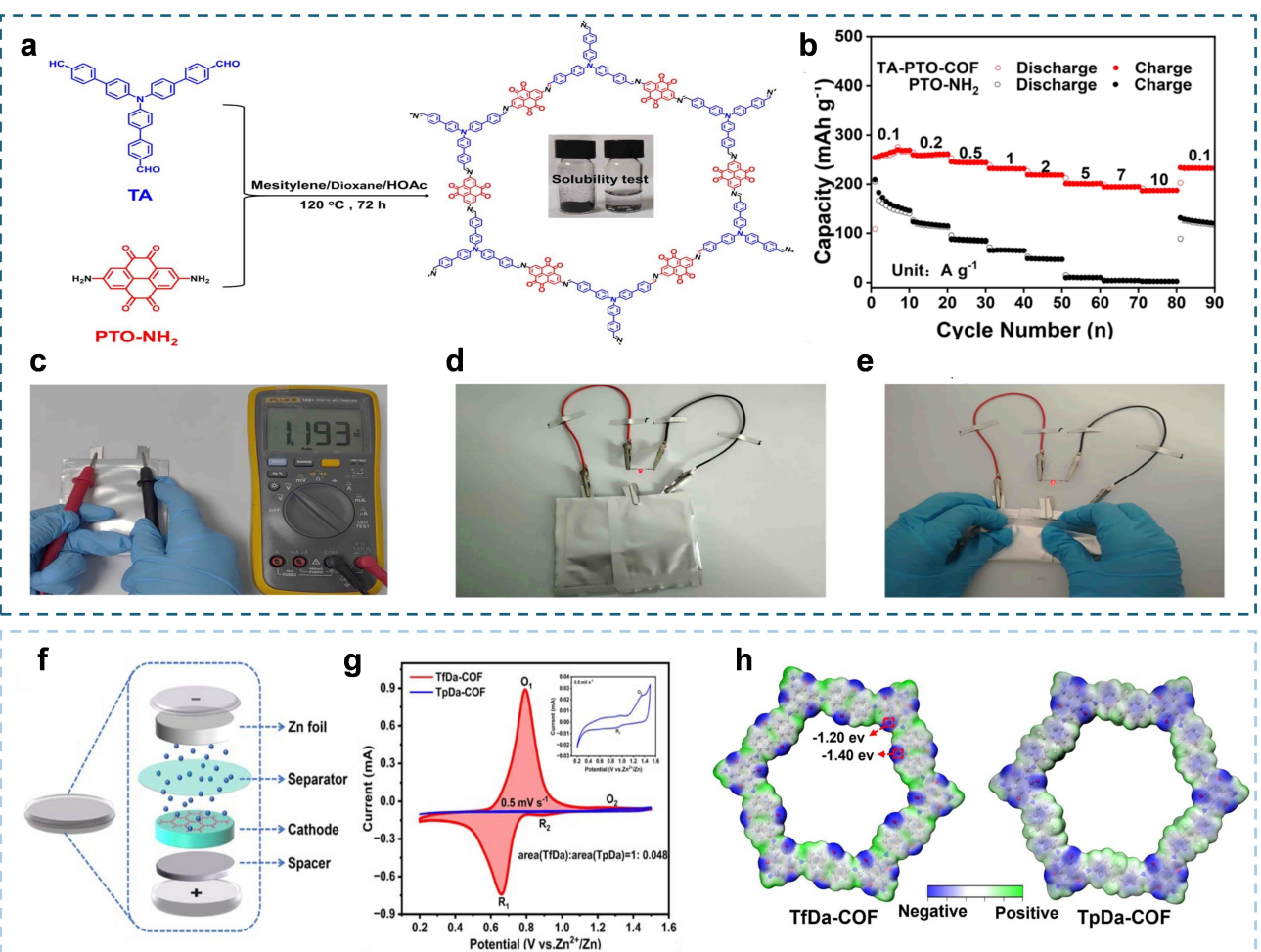


Figure 5. (a) The synthetic pathway for TA-PTO-COF. (b) PTO-NH₂ and TA-PTO-COF rate performances. (c) The pouch cell's open circuit voltage (d and e) image shows different bending angles for pouch cells powering LEDs Reproduced with permission from ref.^[70] 2024 Royal Society of Chemistry. (f) Diagram illustrating the simulation of the Zn//COF-based cell. (g) TpDa-COF and TfDa-COF CV curves under SR 5 mV s⁻¹. (h) Electrostatic potential surface of TfDa-COF and TpDa-COF. Reproduced with permission from ref.^[71] Copyright 2023 Royal Society of Chemistry.

observations underscore the pivotal function of the anthraquinone groups in facilitating Zn²⁺ coordination and in the capacity contributions, which equate to a total of 95.2% of the battery capacity. Moreover, to test the electrochemical performance coin-type cell was used where zinc foil was used as an anode and fiberglass as a separator as shown in Figure 5f. CV profile of TfDa-COF was obtained employing 0.5 mV s⁻¹ of a scan rate (SR). (Figure 5g) Different redox peaks appeared at approximately 0.79/0.66 V, indicative of oxidation and reduction processes attributed to anthraquinone moiety, respectively.

Researchers examined the intercalation mechanism of the TfDa-COF and revealed the formation of O–Zn–O bonds in the layers, facilitated by the binding of C=O groups to Zn²⁺. The MESP (molecular electrostatic potential) analysis of TfDa-COF reveals negative values around the C=O groups (Figure 5h), but TpDa-COF exhibits localized electronegativity primarily around the keto-enol tautomerism carbonyl region. ZIBs using TfDa-COF show favourable capacity performance, achieving a capacity output of 96.6 mA g⁻¹ alongside impressive long-term cyclability with 98% CR at 2.5 A g⁻¹ over 10,000 cycles. The

study presents a promising scheme in improving the performance of COF-based ZIBs.

6.2. Calcium-Ion Batteries (CIBs)

Being the fifth most prevalent element in the Earth's lithosphere, calcium is not only non-toxic but also eco-friendly which makes it feasible for large-scale battery production.^[91] CIBs show great potential but require developments in electrode materials that will enhance the overall electrochemical performance.^[92,93] Researchers are working on numerous strategies to improve its cycling stability, rate capabilities, and the understanding of ion diffusion kinetics. Diversified multi-ion approaches have broadened the spectrum of available active materials suitable for a range of CIB configurations, thereby presenting novel avenues for the realization of superior-performance CIBs.

There has been limited research on COFs for anodic applications, primarily because of their inherently elevated potential, especially when utilized in calcium ion electrolytes.

It's a demanding task to establish low-potential organic anodes, stable, mainly COFs, for CIBs. Wang and colleagues^[28] successfully fabricated PTHAT-COF (Figure 6a) with pyrazine and pyridinamine repeating units through a nucleophilic substitution reaction. Pyridine-2,3,5,6-tetraamine trihydrochloride (Pt) and 1,4,5,8,9,11-hexaazatriphenylenehexacarbonitrile (HAT-CN) have been used as raw materials. PTHAT-COF has been reported as a potential anode material for CIBs. Ultimately, a complete aqueous calcium ion cell was constructed using PTHAT-COF as anode and Mn-PBA in an

aqueous electrolyte (6.67 M CaCl₂). Figure 6b shows a schematic representation of the entire cell along with the practical reaction mechanism. PTHAT-COF anode exhibited sustained structural integrity regardless of undergoing 10,000 cycles with 83.6% of CR, when paired with manganese-based Prussian blue cathode it displayed exceptionally good rate performance of 152.3 mAh g⁻¹. Further mechanistic investigations, including both theoretical and experimental (ex-situ XPS, FT-IR), elucidated the reversible trapping of Ca²⁺ ions by

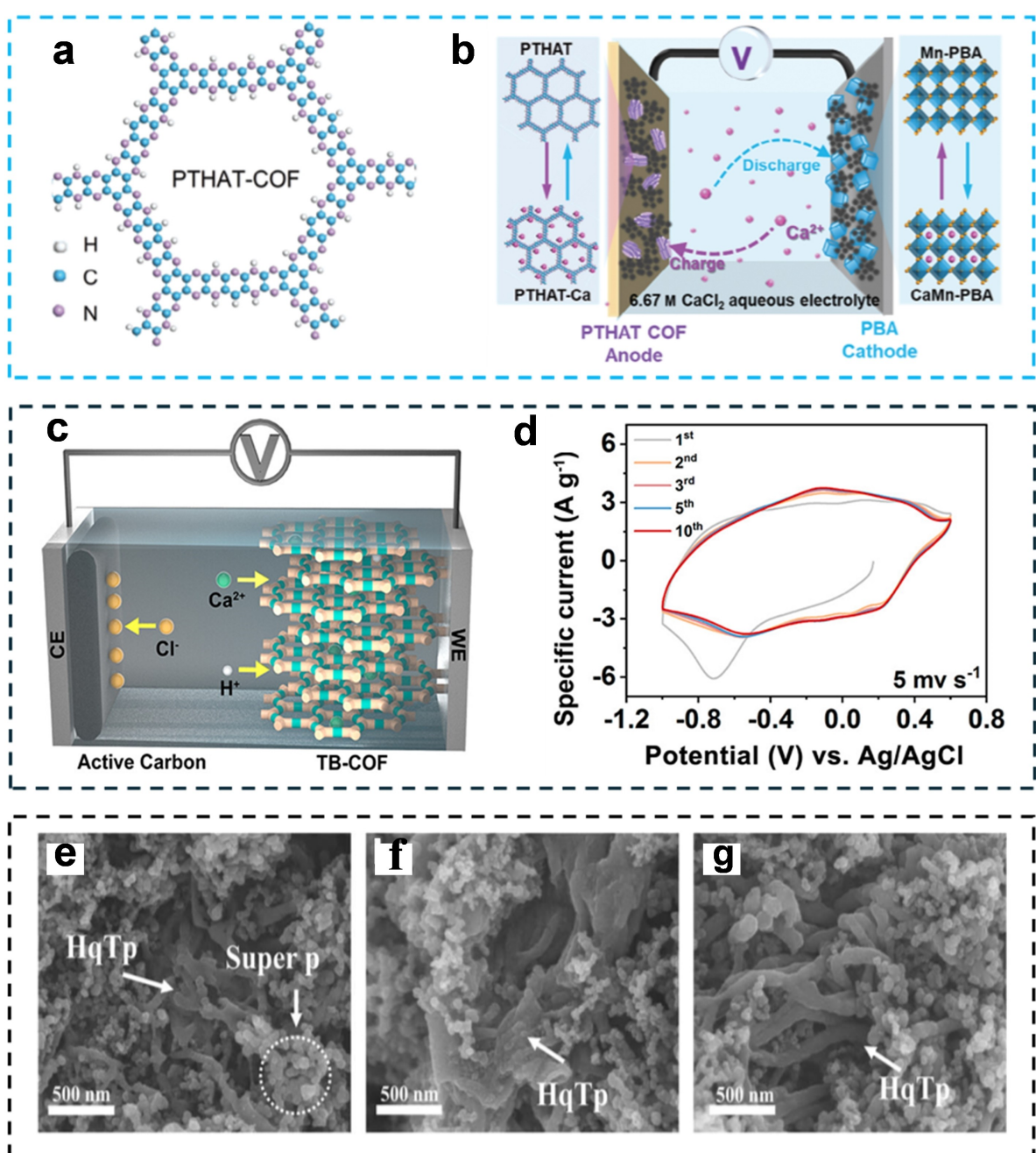


Figure 6. (a) PTHAT-COF's model with ball and stick. (b) Full cell: anode-PTHAT-COF/Cathode-Mn-PBA Reproduced with permission from ref.^[28] 2024 Wiley. (c) Reaction mechanism of TB-COF during the discharge process. (d) Cyclic voltammetry curve at a SR of 5 mVs⁻¹ Reprinted with permission from ref.^[74] Copyright 2023 Journal of the American Chemical Society. HqTp electrodes SEM images: (e) pristine, (f) discharged, (g) charged. Reprinted with permission from ref.^[73] 2022 Royal Society of Chemistry.

C=N active sites through chemisorption mechanisms over the discharge and charging process.

Organic materials exhibit considerable potential as candidates for cation storage within CIBs. Yet, the main issue lies in their tendency to dissolve in electrolytes and their limited ability to conduct electricity, which are critical factors limiting the performance of CIBs. Zhang et al.^[74] fabricated TB-COF which is a nitrogen-rich COF with multiple C=O groups, as an aqueous anode to deal with these hindrances. It was fabricated through a triple condensation reaction involving cyclohexanehexaone (CHHO) and tetraminophenone (TABQ).

One of the key findings reported by the researchers involves distinctive C=C active sites that have been identified within Ca^{2+} ion storage, particularly TB-COF. The range of redox potential of the C=C active site is situated within a lower potential window spanning from -0.5 to -1 V vs Ag/AgCl. The substantiation of the C=C active site's mechanistic role was backed via the observation of radical intermediates during the evolution process. Each repetitive unit of TB-COF can accommodate at most the nine Ca^{2+} ions following three intercalation stages, encompassing three various categories of Ca^{2+} ion storage sites. Since TB-COF has multiple active sites and a minimal presence of inactive components within its framework, TB-COF demonstrates a notably elevated capacity level in the context of reported CIBs. The three-electrode system was used to assess the electrochemical performance of TB-COF. Figure 6c illustrates the battery setup and reaction mechanism. TB-COF served as the working electrode, in which active carbon and Ag/AgCl were put into use as the counter and reference electrodes, respectively. The CV curves (Figure 6d) were recorded at the 5 mVs^{-1} of SR in a span of -1.0 – 0.6 V. Not only does Tb-COF report a high reversible capacity of 253 mAh g^{-1} at 1.0 Ag^{-1} along with enhanced rate performance of 104 mAh g^{-1} at 70 Ag^{-1} but also a sustained cycle longevity, characterized by a nominal capacity degradation of 0.01% per cycle over 3000 cycles at 5 Ag^{-1} .

Lastly, Li et al.^[73] proposed an idea for potential anode material for CIBs. They successfully synthesized a COF material involving 1,3,5-triformamylphloroglucinol (Tp), namely HqTp-COF with a 1.8 nm pore size and 2,5-diaminohydroquinone dihydrochloride (Hq). The mechanism investigation elucidated that rapid charge storage is mainly driven by pseudocapacitance behaviour, contributing over 80% of the overall capacity at a 2 mVs^{-1} SR. Experimental evidence confirmed that carbonyl groups act as reversible electrochemically active sites, enabling the simultaneous insertion of duo Ca^{2+} ions as well as protons. Additionally, an in-situ conversion of C-OH groups to carbonyl groups on HqTp was witnessed, leading to an enhanced SC while both charging and discharging. Moreover, in the scanning electron microscopic (SEM) images, the HqTp with super p nanoparticle morphology and with characteristic nano-strip morphology were seen on the pristine electrode in Figure 6e. Post discharging, the nano-strips became agglomerated and fat (Figure 6f). They reverted back to nano-strips upon charging to 0.8 V vs Ag/AgCl (Figure 6g) demonstrating a reversible behaviour.

The fully assembled cell was made using HqTp as an anode, activated carbon as a cathode, and 1 M CaCl_2 aqueous solution as an electrolyte. It yielded 85.7 mAh g^{-1} of discharge capacity in relation to the mass of HqTp. Over the course of 1600 cycles, the cell exhibited, per cycle, a capacity decay rate of 0.0164% . The HqTp anode demonstrates approximately 109.3 mAh g^{-1} of a SC at 3 Ag^{-1} . Upon increasing the CDs, a specific capacity retention of 65.5% was reported.

6.3. Magnesium-Ion Batteries (MIBs)

MIBs emerge as viable contenders for forthcoming energy storage platforms owing to their elevated theoretical capacity, bivalent characteristics, and the abundant presence of magnesium resources within Earth's natural reservoirs.^[94–96] To overcome the difficulties originated by significant volume fluctuations during cycling, which frequently lead to reduced electrical connectivity and quick capacity degradation, researchers have been developing potential electrode materials for MIBs. Continuous efforts are being made to find the ideal electrode material that satisfies requirements for high capacity, remarkable rate capability, excellent Coulombic efficiency (CE), and long-term cycle stability.

Zou et al.^[76] successfully synthesized quinone-functionalized COF named HAQ-COF (1,4,5,8,9,12-hexaazatriphenylene) for aqueous MIBs. The COF unit comprises standard C=O and C=N functional groups (Figure 7a), utilized as primary active redox sites. The HAQ-COF was utilized as both anode and cathode material, and their respective CRs were approximately 63.5% and 85.6%. During the charge/discharge cycling, the electrochemical polarization progressively escalated, particularly noticeable when employing HAQ-COF as a cathode compared to its usage as an anode. This observation suggested that the augmented electrochemical polarization over cycling primarily accounted for the inferior electrochemical performance observed when HAQ-COF was utilized as a cathode in contrast to its application as an anode. Through the application of diverse ex-situ characterization methods, researchers effectively elucidated the coordination mechanism involving Mg^{2+} responsible for ion storage within the COF. Within a single inner hexagonal COF structure unit, a maximum of 12 Mg^{2+} ions can be coordinated. Electrochemical analysis indicated a predominant pseudocapacitive behaviour during Mg^{2+} ion insertion into COFs. This behaviour effectively mitigates the typically dull solid-phase diffusion issue induced by the enhanced ionic surface charge density of divalent Mg^{2+} ions. HAQ-COF demonstrates an extensive potential window ranging from -0.75 V-to- $+0.75$ V (vs Ag/AgCl). This material achieves 177.4 mAh g^{-1} of SC within the negative potential range (-0.75 – 0 V) and 118.5 mAh g^{-1} within the positive potential range (-0.2 – $+0.75$ V). Leveraging this wide potential window, a symmetric Mg^{2+} ion device was constructed (Figure 7b), yielding 1.5 V of high voltage and a favourable 26.5 Wh kg^{-1} of ED, coupled with an outstanding 3750 W kg^{-1} of PD. Also, practical application potential was

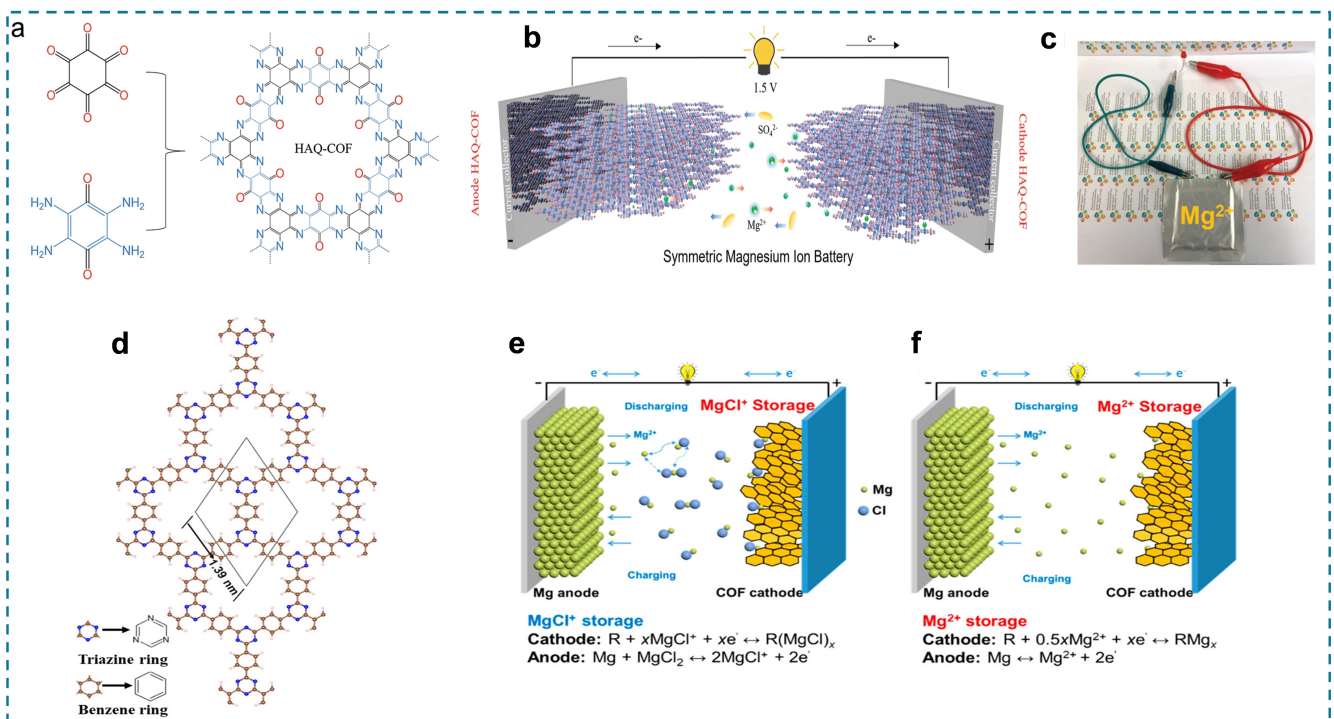


Figure 7. (a) Representation of molecular structure and starting materials of HAQ-COF. (b) Representation of MIB based on COF Reproduced with permission from ref.^[76] 2022 Wiley. (c) Picture of the pouch battery showing powered LED light. (d) Representation of COF with its hexagonal micropore. Representation of equations and reaction mechanism of cathodes in (e) containing chloride, and (f) non-chloride-containing electrolytes Reproduced with permission from ref.^[75] Copyright 2020 American Chemical Society.

shown by employing a symmetric Mg^{2+} ion pouch cell to effectively power an LED (Figure 7c).

Lastly, Sun et al.^[75] reported an outstanding triazine-based COF for MIBs as a cathode material. It was fabricated with the help of a controlled polymerization process of the organic monomer 1,4-dicynobenzene by subjecting it to elevated temperatures in the presence of $ZnCl_2$. Density functional theory (DFT) was utilized to conduct first-principal computation for determining optimized structure. The results revealed the presence of a hexagonal micropore with a diameter of 1.39 nm (Figure 7d). The role of ion storage chemistry significantly influences the specific energy characteristics of batteries. Comparative electrochemical reactions involving $MgCl^+$ and Mg^{2+} storage chemistries in magnesium batteries are illustrated in Figures 7e and 7f respectively. The COF cathode demonstrated 2.8 $kW\text{kg}^{-1}$ of specific power density and a notable 146 Whkg^{-1} of specific energy density. Initially, it exhibited a discharge capacity of 102 mAh g^{-1} at 0.5 C rate (where 1 C equals 114 mAh g^{-1}), while maintaining 70% and 52%. At a discharge rate of 0.2 C, the COF cathode exhibited 107 mAh g^{-1} of discharge capacity. Furthermore, it achieved a reversible capacity of 72 mAh g^{-1} at a high discharge rate of 5 C, with a minimal capacity decay rate of 0.0196% per cycle over 3000 cycles.

6.4. Aluminium-Ion Batteries (AIBs)

AIBs present themselves as highly appealing alternatives for both primary (non-rechargeable) and secondary (rechargeable) applications, owing to their numerous advantageous features. These include the abundant natural occurrence of aluminium, its widespread availability, ease of processing, and cost-effectiveness.^[97,98] However, advancements in AIBs have been relatively slow during the research phase. A primary challenge to address involves the development of cathode materials with the capacity to efficiently store carrier ions containing multivalent aluminium.^[99] Recent developments in AIBs have showcased the promising utilization of COFs as promising cathode materials. COFs, being a novel class of porous materials, demonstrate compelling attributes that render them highly appealing candidates for electrode integration.

Hongyan Lu and colleagues^[79] reported a synthesis of a 2D COF designated TpBpy-COF (Figure 8a) for application as cathode material in AIBs. This COF was synthesized via a condensation reaction involving triformylphloroglucinol (Tp) and 5,5'-diamino-2,2'-bipyridine (Bpy). Notably, TpBpy-COF exhibits a remarkable surface area of 1794 m^2g^{-1} , a value considerably higher than that typically reported for cathode materials or COFs.

Initially, the charge capacity of TpBpy-COF was measured at 152 mAh g^{-1} ; however, it gradually stabilized at 126 mAh g^{-1} upon further discharge. Remarkably, the AIB employing TpBpy-COF as the cathode material maintained a 150 mAh g^{-1}

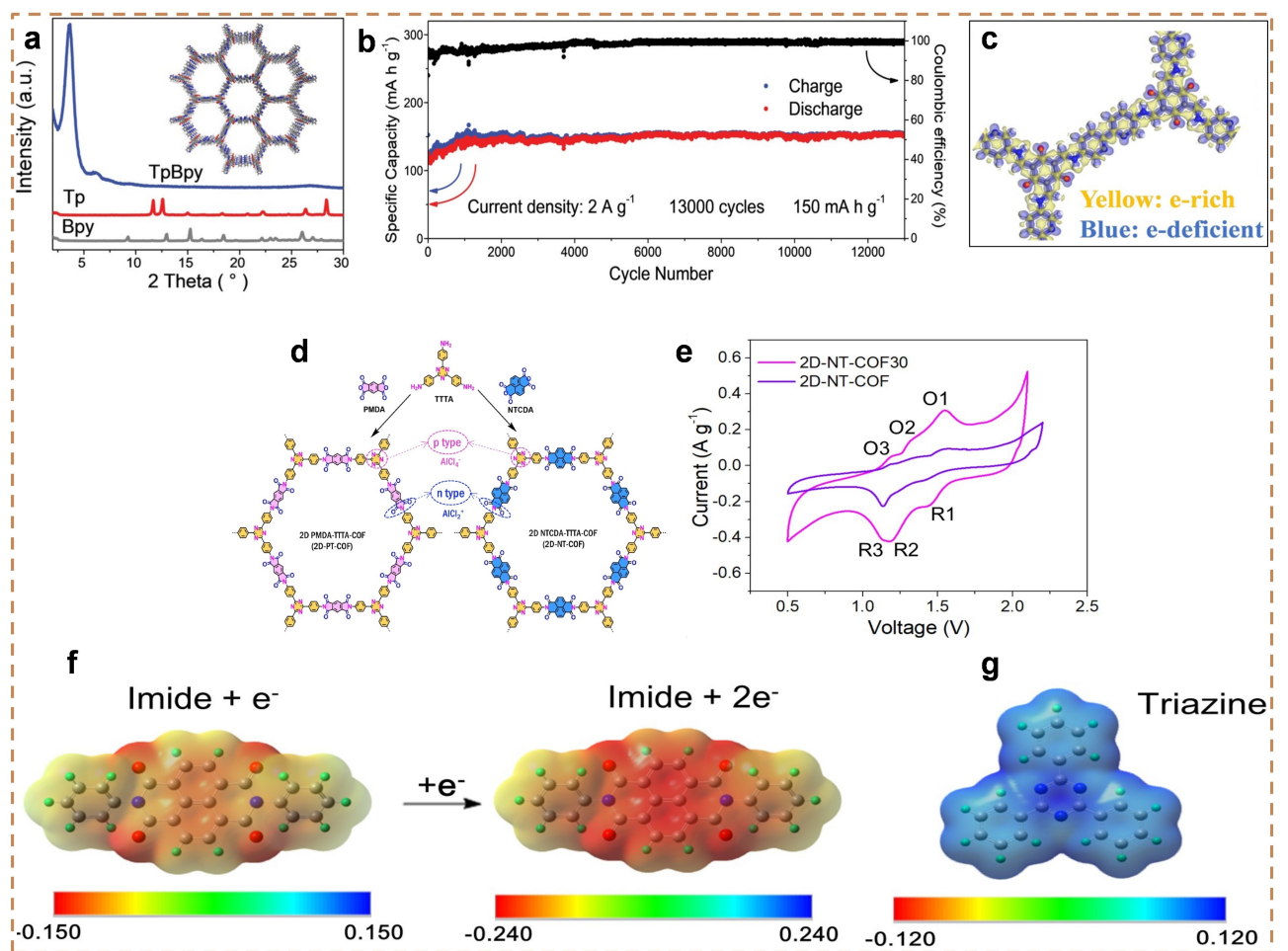


Figure 8. (a) TpBpy-COF PXRD patterns. (b) COF-Al galvanostatic charge-discharge capacities within potential window 0.01–2.3 V Reproduced with permission from ref.^[79] 2020 Wiley. (c) CDD image of TpBpy-COF. (d) Synthetic representation of 2D-PT-COF and 2D-NT-COF. (e) CV profile of 2D-NT-COF30 and 2D-NT-COF at 0.3 mV s⁻¹ of a SR. (f) Representation of imide moieties following the injection of one/two electrons. (g) Representation of triazine after extracting an electron Reproduced with permission from ref.^[100] Copyright 2023 Wiley.

of discharged capacity also demonstrated a CE approaching 100% even over 13,000 cycles at a high CD of 2 A g⁻¹ (Figure 8b), showing long-term stability. To improve the electronic conductivity of the electrode material, carbon nanotubes (CNTs) were incorporated. However, it was observed that CNTs made a trivial contribution (< 20 mAh g⁻¹) to discharge capacity. Figure 8c presents the CDD (charge density difference) for TpBpy-COF where the yellow regions signify regions of electron-rich states, while the blue region indicates areas of electron-deficient states. This research showed the potential of TpBpy-COF as a high-performance cathode material for AlIBs, offering both substantial surface area and exceptional long-term stability. The findings of this research also provide insights into the limited impact of CNTs on the discharge capacity of composite electrodes.

Addressing the challenges for high-performance cathode materials, Liu and colleagues^[100] investigated redox-bipolar 2D COFs for AlIBs. They reported the synthesis pathway of polyimide 2D COFs involving the monomers of 4,4',4''-(1,3,5-triazine-2,4,6-triyl)trianiline (TTA) and pyromellitic dianhydride (PMDA), named 2D-PT-COF, and between TTTA and

1,4,5,8-naphthalene tetracarboxylic dianhydride (NTCDA), named 2D-NT-COF (Figure 8d). Both electrodes CV curves, 2D-NT-COF and 2D-NT-COF30 (in-situ grown on CNT) were observed at the 0.3 mV s⁻¹ of SR as shown in Figure 8e. Both materials showcase the redox-bipolar characteristics by incorporating p-type and n-type imide triazine groups within a single framework. As a result, 2D-NT-COF demonstrates a substantial 132 mAh g⁻¹ of SC, which indicates 80.5% elevated active site utilization efficiency. The electrode also displayed ultralong cycling stability with over 97% CR after 4000 cycles, equivalent to a mere 0.0007% capacity decay per cycle.

The researchers conducted calculations to access the MESP (molecular electrostatic potential) of the electron-injected imide groups of 2D-NTCOF, as illustrated in Figure 8f, along with the triazine moiety after the removal of an electron, shown in Figure 8g.^[101,102] In the imide moieties with one and two electrons injected, the oxygen atoms of the imide exhibit the lowest electrostatic potential, indicating their tendency to act as nucleophilic sites for cation binding. On the other hand, the nitrogen atoms of the triazine moiety display the highest electrostatic potential upon extraction of an electron, suggest-

ing their role as electrophilic sites potentially involved in binding atoms. CNTs have been used to elevate the charge transport capability with a COF/CNT mass ratio of 7:3 and the resulting hybrid materials were labelled as 2D-PT-COF30 and 2D-NT-COF30 respectively. Findings indicated that CNTs had a significant contribution in enhancing charge transport of the 2D-NT-COF30 and demonstrated exceptional electrochemical performance.

7. Applications of COFs as Separators in Batteries

A battery consists of four main parts that include the anode, cathode, electrolytes, and separators. Separators play a crucial role within the battery system, exerting a critical influence on its electrochemical performance. Primarily, the separator serves to function as a physical barrier between the cathode and anode electrodes, effectively mitigating the potential hazards associated with short-circuiting by averting direct contact.^[103,104] The presently employed polyolefin-based separators, notably polypropylene (PP) and polyethylene (PE) are characterized by robust mechanical properties and commendable chemical and electrochemical resilience.^[105] However, their wettability and thermal stability fall short of the desired standards.^[106,107] To overcome such obstacles, exciting research is underway on COF-based separators, demonstrating outstanding separation capabilities that promise to revolutionize various applications.

An idea for an enhanced separator was proposed by Min et al.,^[108] introducing COF into poly(arylene ether benzimidazole) (OPBI) for LIBs. SNW-1 (Schiff-based network –1) was used as nanoparticles incorporated into the OPBI polymer to prepare OPBI@COF by using the NIPS (non-solvent induced phase separation) method, which helped to improve properties such as high porosity, impressive thermal stability, high ionic conductivity, good flexibility, and improved electrolyte wettability. The inclusion of SNW-1 within composite separators significantly improved their efficiency in preventing the enlargement of lithium dendrites, facilitating lithium electrodeposition, and augmenting the overall efficiency and safety of LIBs, particularly under elevated temperatures.

Researchers prepared different OPBI composite separators with diverse COF contents of 10 and 20 wt % by incorporating SNW-1 nanoparticles and named as OPBI@COF10 and OPBI@COF20, respectively. The implementation of OPBI@COF composite separators led to a notable enhancement in performance metrics relative to conventional PP separators. Specifically, cells equipped with PP and OPBI@COF20 separators exhibited CR rates of 96.6% and 99.0%, respectively. Moreover, the CE remained consistently high, ranging between 99% and 100% for cells utilizing both types of separators. The LiFePO/Li cell, integrated with the OPBI@COF20 separator, demonstrated a 148.3 mAh g^{-1} of specific discharge capacity. Remarkably, its 99% CR was followed by 200 cycles at a rate of 0.5 C.

Another study on the enhancement of the separator was done by Yao et al.^[109] A strategy including positively charged organic units and loosely bounded fluoride ions (F^-) was incorporated in COF to alter the conventional polypropylene separator, resulting in COF–F@PP modification for lithium metal batteries (LMBs). The COF was synthesized via Schiff reaction where TG_{Cl} (triaminoguanidinium chloride) and Dha (2,5-dihydroxyterephthalaldehyde) were mixed with another solution containing deionized water and 1,4-dioxane (Figure 9a). Applying coating layers onto the dual surfaces of the commercial PP separator through a straightforward blade-coating technique involves utilizing COF-bounded Cl^- ($\text{COF}-\text{Cl}$) within its porous structure. This COF–Cl demonstrates promising capabilities in facilitating the transportation and modulation of lithium ions owing to its unique capacity to immobilize ionic centres and binds ion guests, and it is used as a comparison material to COF–F@PP to evaluate the performance of modified separators. The substitution of Cl^- with F^- in the COF (COF–F) occurs via an ion exchange reaction. This process facilitates the generation of SEI (solid electrolyte interphase) rich in LiF over the surface of the anode. The resulting SEI layer serves to mitigate side reactions and suppress dendrite formation, contributing to elevated battery performance and stability (Figure 9b). The Li//LFP battery employing COF–F@PP as a separator displayed robust cycling performance, sustaining 450 cycles at 1 C and 2000 cycles at 5 C, with notable retention of capacity and CE. Remarkably, both pouch cell and N/P ratio full cell, with COF–F@PP show exceptional cycling stability and rate capability, underscoring the considerable commercial potential of the modified separator.

An interesting study on a design methodology aimed at emulating both the structural arrangement and operations principles of human cerebral blood vessels in the fabrication of an optimal separator for sodium-sulfur (Na–S) batteries was done by Chen and colleagues.^[110] Drawing inspiration from the physiological mechanisms of human cerebral blood vessels, researchers engineered a bilayer separation for Na–S batteries. This separator incorporates three key functional elements: 1) Ionic molecules, 2) COFs, and 3) CNTs. The resulting biomimetic membrane is denoted as HB/CNT@COF, where HB is hydroxynaphthol blue, and features well-defined sodium ion-selective movement pathways and polysulfide switching layers. To enhance the effectiveness of the framework, COF-300, characterized by 7.2 \AA^0 pores and notable chemical stability, was selected as the foundation matrix for anchoring. The encapsulation of CNTs and HB within the COF-300 membrane was achieved through in-situ self-assembly and due to synergistic interaction between both, the HB/CNT@COF cell displayed a 733.4 mAh g^{-1} of capacity with minimal capacity degradation observed over 400 cycles at 4 C. Additionally, the HB/CNT@COF cell, employing an electrolyte-to-sulfur ratio (E/S) of 10 mL g^{-1} , retains a 922.3 mAh g^{-1} of capacity over hundred cycles at 0.1 C.

Shi et al.^[111] successfully synthesized an imide-based COF, formed from a reaction involving 1,3,5-triformylphloroglucinol (TFP) and paraphenylenediamine, named COF-TpPa and sub-

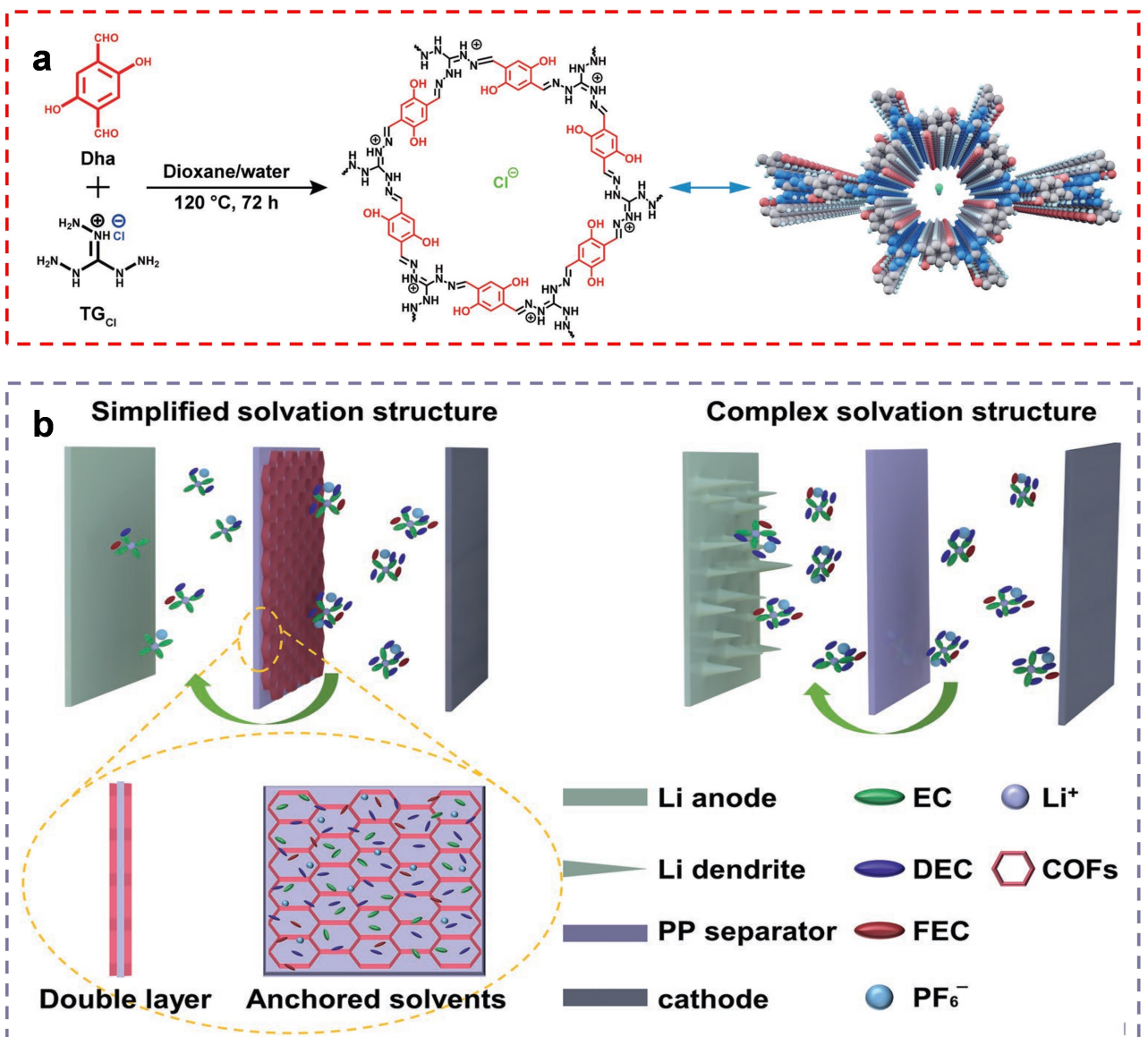


Figure 9. (a) Representation of synthetic route of COF-Cl. (b) graphical representation and comparison with batteries with different separators: left- COF-f@PP and right- pristine pp. Reprinted with permission from ref.^[109] Copyright 2023 Wiley.

sequently integrated with reduced graphene oxide (rGO) via an O₂ free solvothermal method (Figure 10a). The interaction between amide and aldehyde functionalities within TFP and p-phenylenediamine was guided by the presence of rGO nanosheets, leading to the nanosheets generation of COF-TpPa. Additionally, employing a straightforward solvothermal method allowed for easy modification of the channel surface of COF-TpPa through the alteration of monomer functional groups. By utilizing 2-chloro-p-phenylenediamine/2,5-diaminobenzenesulfonic acid as monomers, COF-TpPa-Cl@rGO or COF-TpPa-SO₃H@rGO hybrid nanosheets with distinct functionalities were fabricated. When utilized in the separator in LIBs, the COF-TpPa-SO₃H@rGO demonstrates substantially improved performance metrics, including 1163.4 mAh/g of high SC at 0.2 C along with 60.2% of long cyclic stability retention over 1000 cycles at 2.0 C.

A self-standing COF separator (TPB-BD(OH)₂-COF) renamed as COF/PVDF was fabricated and employed as a separator in LMBs by Yang et al.^[112] COF/PVDF was engineered by incorporating an extremely thin layer of PVDF onto a constant and a COF membrane that was seemingly defect-free. The addition of PVDF is solely intended to enhance the flexibility of the separator. As observed from Figure 10b, during the migration of lithium-ion solvent sheath from one electrode side to the anode, it'll have to go through the separator. In the absence of additional costly lithium salts and additives, hydrogen bonding interactions can occur among the hydroxyl groups (OH⁻) present in the COF/PVDF separator and the components of the diluted electrolyte, such as —OH···F (—OH/PF₆⁻) and —OH···O (—OH/EMC). This interaction facilitates a reduction in the excess of free molecules within the sheath of lithium-ion solvent, owing to the affinity among diluted electrolyte

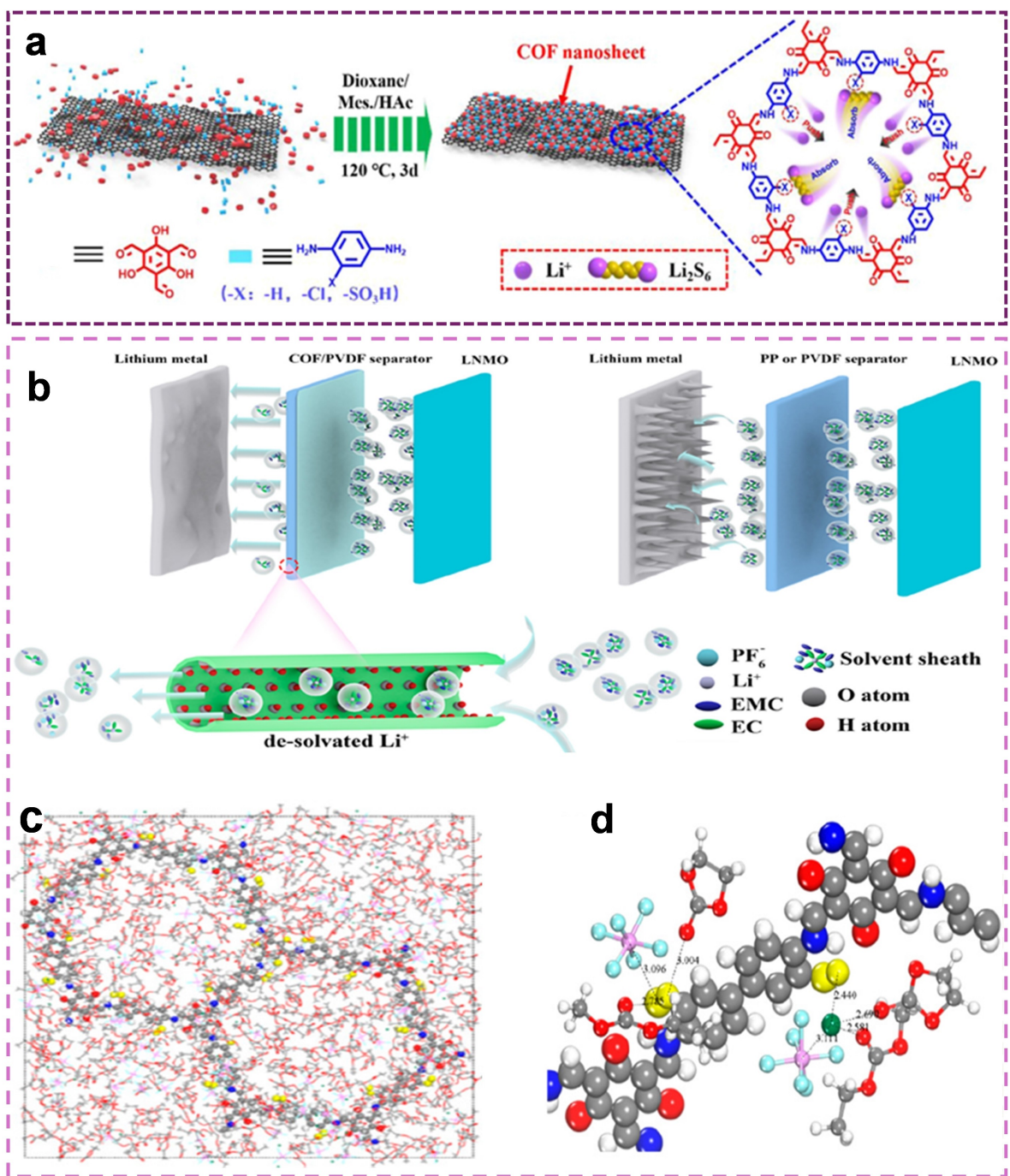


Figure 10. (a) Representation of synthetic pathway of COF-SO₃@rGO Reprinted with permission from ref.^[111] Copyright © 2022 American Chemical Society. (b) left- COF/PVDF separator electrolyte, including lithium-ion deposition; right- electrochemical behavior of diluted electrolyte in conventional separator (PP or PVDF). (c) MD snapshot displaying the solvated shell of Lithium ions within COF. (d) Representation of MD model of COF. Reproduced with permission from ref.^[112] Copyright 2022 American Chemical Society.

components and COF. The whole electrolyte transport occurs within the channels of the COF, wherein the COF serves as a protective barrier for the electrolyte. Additionally, combustion experiments confirmed the exceptional flame-retardant properties of the COF/PVDF separator towards the electrolyte indicating its suitability for use in high-temperature environments. The limitations of DFT calculations in capturing interactions between multiple components necessitate em-

ploying force field-based molecular dynamics (MD) methods to elucidate the hydrogen bond network involving hydroxyl functional groups in COF/PVDF channels and anions or solvent molecules in the electrolyte. A model of dimensions 6.5×6.5×4.5 nm³ shown in Figure 10c, allows for a more intuitive observation of electrolyte dynamics. MD simulations were conducted to examine the solvated shell surrounding the Li-ion inside a radius of 5 Å, as displayed in Figure 10d.

This snapshot was extracted from a specific 4 ns MD trajectory for analysis. The device assembled using the fabricated separator displayed 700 h of stable cycling at a CD of 1 mA cm^{-2} . Utilizing this separator, a lithium metal anode having SC of 5 mAh cm^{-2} , and a high-voltage LNMO cathode, the assembled full battery maintains a specific discharge capacity of 129.2 mAh g^{-1} over 200 cycles at a CE of 0.5 C, with a remarkable CR ratio of 98.8%.

Research focusing on separators within Na–S batteries is notably uncommon when contrasted with the extensive investigation efforts directed toward the electrodes. The separator, recognized as a pivotal component within Na–S batteries, functions as an insulating barrier between electrodes while facilitating the transport of cations. Na–S batteries experience rapid degradation of cell capacity and limited lifespan due to the significant challenges posed by the polysulfide shuttle phenomenon and inactive redox kinetics, working on this issue Yin et al.^[113] successfully fabricated a potential separator for Na–S batteries using 1,3,5-triformylbenzene and azobenzene-modified hydrazide linkers (Azo-Th), denoted as Azo-TbTh. Hydrazine monomers featuring branched azobenzene side groups undergo a reaction with aldehydes, yielding the formation of COF thin films characterized by narrowed pores that are adorned with azo functionalities. One aspect involves the azobenzene side groups, which reduce the pore diameter to sub-nanometre dimensions, effectively hindering the polysulfide shuttle. Conversely, these groups create ion-hopping sites along the directionally aligned nanochannels, thereby enhancing the migration of Na^+ ions by reducing transport resistance^[114–116](Figure 11a–b). The synergic effect of azo groups incorporated into the COF pore walls leads to the effective blocking of polysulfide migration while simultaneously aiding the transport of Na^+ ions. As a result, Na–S batteries utilizing this COF fine layer as the separator demonstrate remarkably elevated rate performance, SC, and 0.036% of an ultra-low attenuation rate per cycle over 1000 cycles. CV curves are shown in Figure 11c where the spanning of the SR was 0.5–2.8 V. Moreover, as illustrated in Figure 11d, researchers showed that the structural integrity of the Azo-TbTh separators remains uncompromised following folding and subsequent recovery into quarters, thereby indicating its exceptional foldability and flexibility.

Working on a similar issue in lithium-sulfur (Li–S) batteries, Xu et al.^[117] fabricated a potential separator material named SCOF-2, dual sulfonate-rich COF. The fabrication was done using a Schiff-base reaction between 2,4,6, -trihydroxybenzene-1,3,5-tricarbaldehyde and 2,5-diaminobenzene-1,4-disulfonicacid.^[118,119] Through substitution of the sulfonated building block with benzene-1,4-diamine or 2,5-diaminobenzenesulfonic acid, analogous structures to the non-sulfonated COF (TpTa-COF) and mono sulfonated COF (SCOF-1) were synthesized to facilitate comparative analysis. SCOF-2 functionalized with a high concentration of sulfonic groups, serves as an ionic sieve capable of repelling polysulfide anions, concurrently facilitating Li^+ ion migration (Figure 11e), and absorbing molecular LiPSs. Comparative analysis with mono-

sulfonated/nonsulfonated COFs reveals that SCOF-2 exhibits enhanced electronegativity and expanded interlayer spacing. These properties not only impede polysulfide migration but also mitigate the generation of Li-dendrites. When contrasted with the pristine PP separator, the electronegative SCOF can obstruct unwanted polysulphide species while facilitating the selective permeation of Li^+ ions. This feature serves to safeguard the Li anode from corrosion, as outlined in Figure 11f. SCOF-2 exhibited notable performance metrics, including 479 mAh g^{-1} of a high-rate capacity at 5 C current, a remarkably low 0.047% attenuation rate per cycle even after 800 cycles at 1 C, and an outstanding anti-self-discharge characteristic, with only 6.0% capacity decrease over one week of rest. Additionally, it demonstrated 4.92 mAh cm^{-2} of a reversible capacity and maintained CR of 81.2% over 100 cycles, obtained through the conditions of 8.2 mg cm^{-2} sulphur loading and $5 \mu\text{l mg}^{-1}$ lean electrolyte. These results surpass the performance of the majority of the other COF materials utilized in Li–S batteries.

8. Strategies to Improve the Electrochemical Performance of COF in Battery Systems

COFs are emerging materials that can play a key role in enhancing the performance of energy storage systems, particularly in improving working voltage. The voltage of COF-based electrodes is intrinsically tied to their molecular structure, especially the redox-active linkages that determine electron transfer during charge and discharge cycles. COF materials can be broadly classified into n-type, p-type, and bipolar-type, each offering distinct voltage characteristics based on their redox mechanisms.

For p-type COFs, the redox process involves the conversion between neutral and positive states, which generally provides a higher working voltage and this is attributed with the Highest Occupied Molecular Orbital (HOMO). However, this requires a substantial amount of electrolyte to balance charges, which reduces energy density and poses challenges for practical applications. In contrast, n-type COFs, where the voltage is determined by the Lowest Unoccupied Molecular Orbital (LUMO), offer a more stable pathway for enhancing discharge voltage. By introducing electron-withdrawing groups, the LUMO energy level can be lowered, thereby increasing the voltage. Conversely, electron-donating groups can reduce the LUMO energy level, adjusting the voltage downward. This tunability is a key advantage of n-type COFs for battery design.^[120]

Moving forward, the design of COFs with redox-active linkages such as $\text{C}=\text{O}$ and $\text{C}=\text{N}$ groups has shown a great promise due to their ability to deliver high capacities and moderate working voltages, along with exceptional cycling stability. The development of new n-type linkages with higher electron affinities and larger π -conjugated structures are crucial for further increasing working voltage. Furthermore, computational approaches, such as theoretical simulations,

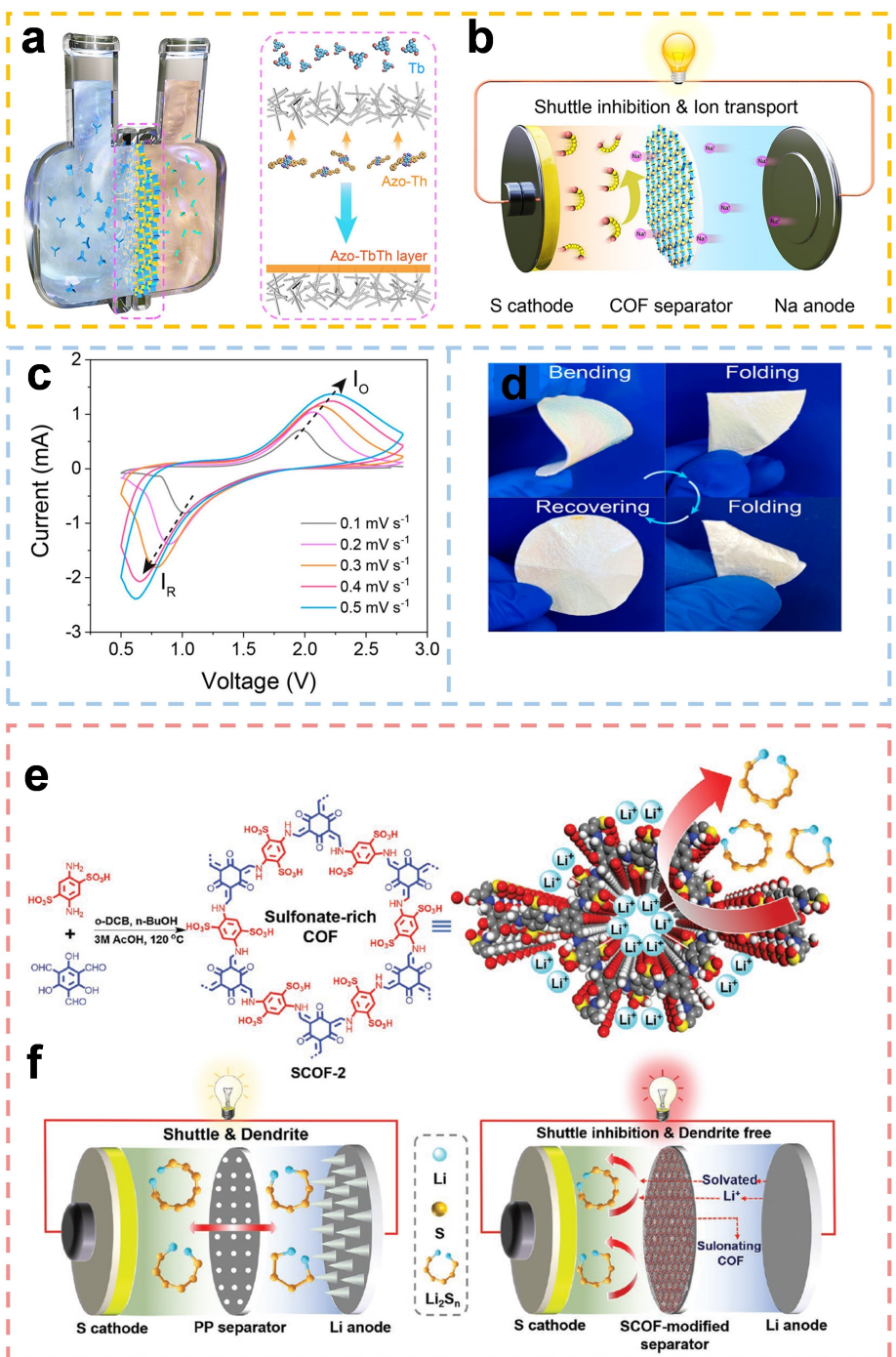


Figure 11. Graphical representation of (a) azobenzene-branched COFs synthetic route with selective transport of sodium ion and (b) Na-S battery with separator based on COF. (c) CV curves at various scan rates. (d) Pictures displaying Azo-TbTh separator's flexibility Reproduced with permission from ref.^[113] Copyright © 2022 American Chemical Society. (e) Fabrication route of sulfonated COF. (f) Comparison using different separators- (left) PP/right-SCOF Reprinted with permission from ref.^[117] Copyright 2021 Wiley.

can aid in optimizing molecular structures, predicting redox behaviour, and guiding the synthesis of COF materials tailored for improved voltage performance.^[56,57] Ultimately, COF-based electrolyte materials hold significant potential to elevate the working voltage of next-generation batteries, particularly for multivalent ion batteries by combining high electron/ion transfer efficiency with enhanced redox activity.

9. Approaches to Achieve Target COFs

The development of COFs has attracted significant attention in recent years because of their highly defined and diversified structures, which facilitate the study of structure-performance relationships. This is particularly valuable for exploring catalytic mechanisms and designing new COFs for various func-

tional applications. The inherent flexibility in tailoring COF structure presents ample opportunities to design various functional materials tailored for specific applications. Generally, two principal approaches exist for structural modulation: bottom-up and post-synthetic modification. The bottom-up strategy involves the preferential design of monomers to directly synthesize targeted COFs. At the same time, post-synthetic modifications introduce new functional groups into pristine COFs, allowing for adjustments to their surface or pore environments without altering the original framework. This expands the potential application of COFs significantly.^[62]

In addition to post-synthetic metalation, COF structures can be further tuned by incorporating additional functional groups, enhancing their properties and functionalities. Various techniques have been developed to facilitate the integration of these functional groups, focusing on improving physicochemical properties, tunable porosity, cost-effective synthesis, and desirable characteristics.^[57] Crucially, the creation of highly ordered and crystalline COFs necessitates careful consideration of the preparation pathway, including factors such as the choice of reaction medium, temperature, time, and catalysts. To develop well-ordered crystalline COFs for electrode materials, a solid understanding of the construction units, synthetic routes, and thermodynamic equilibria governing covalent bonding is essential.^[121] This comprehensive approach not only advances the design of COFs but also enhances their performance in electrode applications, paving the way for innovative energy storage and conversion technologies.

10. Conclusions and Future Perspectives

COFs are crystalline materials in 2D, and 3D structures known for their porosity and integration of individual building units, resulting in diverse and expanded framework structures. COFs, as a series of polymers, possess unparalleled extended frameworks whose topological arrangements are able to be anticipated and designed through specific combinations of building blocks. They have emerged as fascinating materials with distinct characteristics that make them outstanding candidates for energy storage applications. Traditionally, COFs have been primarily synthesized through the solvothermal method, but recent research has explored alternative approaches aiming for enhanced convenience in fabricating COFs, opening doors to exciting possibilities in COF research. COFs show exceptional performance in multivalent ion batteries (ZIB, CIB, MIB, and AIB) but still, there are relatively fewer reports available on COFs being used as electrode or separator materials and needs to be explored.

The evolution of COF development is currently in its preliminary phases, with numerous challenges yet to be addressed. This review offers an overview of the various complexities and potential pathways for future exploration within this discipline. The fabrication of COF materials is mostly done via the solvothermal method which often necessitates prolonged durations or elevated temperatures, rendering them less suitable for large-scale production. While the microwave method offers relatively shorter reaction times but still its scalability remains a

major challenge. Thus, there is a pressing need to investigate alternative linkage reactions combined with more accessible synthetic methodologies for COF synthesis. The electrochemical redox centre fundamentally influences the capacity performance of COF electrodes. Clearly, enhancing both the quantity and diversity of active centres within the constituent building blocks serves as an initial step in the conceptualization of novel electrode material. Investigating novel active groups derived from existing ones and enhancing their utilization efficiency through strategic adjustments in their spatial arrangement, are crucial considerations in this pursuit. However, tailoring the chemical composition of COF materials to optimize redox-active sites, encompassing functionalization with specific groups that promote redox reactions and ion interactions, presents a viable solution.

High levels of ionic and electronic conductivity are recognized as crucial factors influencing the rate capability of electrode materials. However, the notable limitation of lessened electrical conductivity poses a significant challenge for practical applications of COFs in electrochemical energy storage. At the core of this challenge lies the fundamental design principle of incorporating π -conjugated skeleton into COF materials to enhance conductivity. Additionally, the crystalline structures characterized by robust interactions between layers also contribute significantly to electron conductivity. Not only that but also through the introduction of highly conductive graphene oxide, metal oxide, CNTs,^[79] and conductive polymers, considerable enhancements have been achieved.^[122,123] Even, engaging in the advancement of COF materials with intrinsic conductivity is a promising proposition. Despite the extensive literature on the utilization of COFs in electrochemical and energy storage applications, the underlying mechanisms remain inadequately defined. A thorough understanding of storage mechanisms and identification of emerging intermediates while charge-discharge cycles are very crucial for the enhancement of multivalent ion batteries. The integration of sophisticated in-situ characterization techniques and computational studies can provide deeper insights into the real electrochemical processes, enhancing their credibility.

Amidst the electrode preparation, the grinding process poses a risk of damaging the anisotropic packing of COF crystallites. Hence, optimizing the precise size and configuration control of COF material demands rigorous efforts. Structure collapse often emerges as the primary cause of electrode failure. Therefore, it becomes necessary to ascertain the preservation of COF's crystallinity when organic building blocks undergo oxidation and reduction amidst the charge/discharge cycle. The presence of redox-active sites exhibiting energy storage activity, such as C=N, carbonyl group, triazine rings, and benzene rings significantly enhances the ED of materials based on COF. Notably, effective utilization of energy storage active groups like triazine rings and benzene rings within COF structure leads to substantially higher capacities compared to COFs relying solely on carbonyl and imine group functional energy storage mechanisms.

In the ZIBs, the advent of self-charging batteries heralds a promising frontier, yet the absence of a standardized evaluation pathway for examining the self-charging performance of cathode materials remains a significant gap in research. Exploring methodologies to gauge parameters such as self-charging efficiency and

average self-charging rate holds considerable promise to comprehensively evaluate the efficacy of these materials.^[67]

Exploring fundamental challenges and mitigating constraints associated with surface modification techniques for the effective implementation of modified separators in practical applications. The coating process unavoidably leads to an augmentation in separator thickness, thereby impeding the ionic conductivity of modified separators by introducing additional interfaces between the separator substrates and coating materials. Hence there is a critical need to conduct fundamental investigations to elucidate the interfacial bonding dynamics between the coating material and COF separator, alongside the preservation of the porous structure of the separator, which enhances its thermal stability.

In summary, the field of energy storage materials COF continues to present ample opportunities for further research and advancements. Researchers have made notable progress in achieving novel COFs with diverse functionalities, precise structures, and enhanced performances. Additionally, should COFs exhibit favourable electrochemical and mechanical properties, they hold the potential to replace both separator and electrode materials in relevant applications.

Acknowledgements

VS is thankful to the Vellore Institute of Technology (VIT) for allowing overseas research attachment at QUT. The authors are grateful to the Central Analytical Research Facility (CARF) at Queensland University of Technology.

Conflict of Interests

The authors declare no conflict of interest.

Keywords: Covalent Organic Frameworks (COFs) • Multivalent Metal-Ion Batteries (MMIBs) • Separators • Electrochemical performance

- [1] V. S. Vyas, F. Haase, L. Stegbauer, G. Savasci, F. Podjaski, C. Ochsenfeld, B. V. Lotsch, *Nat. Commun.* **2015**, *6*, 8508.
- [2] C. R. Mulzer, L. Shen, R. P. Bisbey, J. R. McKone, N. Zhang, H. D. Abruna, W. R. Dichtel, *ACS Cent. Sci.* **2016**, *2*(9), 667–673.
- [3] H. Xu, J. Gao, D. Jiang, *Nat. Chem.* **2015**, *7*(11), 905–12.
- [4] A. P. Cote, A. I. Benin, N. W. Ockwig, M. O’Keeffe, A. J. Matzger, O. M. Yaghi, *Science* **2005**, *310*(5751), 1166–1170.
- [5] X. Feng, X. Ding, D. Jiang, *Chem. Soc. Rev.* **2012**, *41*(18), 6010–22.
- [6] O. Yahiaoui, A. N. Fitch, F. Hoffmann, M. Froba, A. Thomas, J. Roeser, *J. Am. Chem. Soc.* **2018**, *140*(16), 5330–5333.
- [7] P. J. Waller, F. Gandara, O. M. Yaghi, *Acc. Chem. Res.* **2015**, *48*(12), 3053–63.
- [8] F. Haase, B. V. Lotsch, *Chem. Soc. Rev.* **2020**, *49*(23), 8469–8500.
- [9] M. Chafiq, A. Chaouiki, Y. G. Ko, *Energy Storage Mater.* **2023**, *63*.
- [10] C. S. Diercks, O. M. Yaghi, *Science* **2017**, *355*(6328).
- [11] S. Wan, F. Gándara, A. Asano, H. Furukawa, A. Saeki, S. K. Dey, L. Liao, M. W. Ambrogio, Y. Y. Botros, X. Duan, S. Seki, J. F. Stoddart, O. M. Yaghi, *Chem. Mater.* **2011**, *23*(18), 4094–4097.
- [12] C. Jiang, M. Tang, S. Zhu, J. Zhang, Y. Wu, Y. Chen, C. Xia, C. Wang, W. Hu, *Angew. Chem. Int. Ed. Engl.* **2018**, *57*(49), 16072–16076.
- [13] J. Zhou, B. Wang, *Chem. Soc. Rev.* **2017**, *46*(22), 6927–6945.
- [14] M. S. Lohse, T. Bein, *Adv. Funct. Mater.* **2018**, *28*(33).
- [15] Y. Song, Q. Sun, B. Aguila, S. Ma, *Adv. Sci. (Weinh.)* **2019**, *6*(2), 1801410.
- [16] S. Y. Ding, W. Wang, *Chem. Soc. Rev.* **2013**, *42*(2), 548–68.
- [17] X. Zhao, P. Pachfule, A. Thomas, *Chem. Soc. Rev.* **2021**, *50*(12), 6871–6913.
- [18] C. Wang, J. Tang, Z. Chen, Y. Jin, J. Liu, H. Xu, H. Wang, X. He, Q. Zhang, *Energy Storage Mater.* **2023**, *55*, 498–516.
- [19] C. Jiang, Y. Gu, M. Tang, Y. Chen, Y. Wu, J. Ma, C. Wang, W. Hu, *ACS Appl. Mater. Interfaces* **2020**, *12*(9), 10461–10470.
- [20] N. K. Sahu, A. K. Nayak, A. N. Grace, *Materials for Energy Storage*. CRC Press, Taylor & Francis Group: **2024**.
- [21] C. Li, L. Liu, J. Kang, Y. Xiao, Y. Feng, F.-F. Cao, H. Zhang, *Energy Storage Mater.* **2020**, *31*, 115–134.
- [22] X. Gao, Y. Dong, S. Li, J. Zhou, L. Wang, B. Wang, *Electrochem. Energy Rev.* **2019**, *3*(1), 81–126.
- [23] J. Chu, Y. Wang, F. Zhong, X. Feng, W. Chen, X. Ai, H. Yang, Y. Cao, *EcoMat* **2021**, *3*(5).
- [24] H. Zhang, Y. Geng, J. Huang, Z. Wang, K. Du, H. Li, *Energy Environ. Sci.* **2023**, *16*(3), 889–951.
- [25] M. Wu, Y. Zhao, R. Zhao, J. Zhu, J. Liu, Y. Zhang, C. Li, Y. Ma, H. Zhang, Y. Chen, *Adv. Funct. Mater.* **2021**, *32*(11).
- [26] B. C. Patra, S. K. Das, A. Ghosh, K. Raj, A. P. Moitra, M. Addicoat, S. Mitra, A. Bhattacharyya, A. Pradhan, *J. Mater. Chem. A* **2018**, *6*(34), 16655–16663.
- [27] J. Lee, H. Lim, J. Park, M. S. Kim, J. W. Jung, J. Kim, I. D. Kim, *Adv. Energy Mater.* **2023**, *13*(26).
- [28] C. Wang, R. Li, Y. Zhu, Y. Wang, Y. Lin, L. Zhong, H. Chen, Z. Tang, H. Li, F. Liu, C. Zhi, H. LvA, *Adv. Energy Mater.* **2023**, *14*(1).
- [29] J. Sun, Y. Fei, H. Tang, J. Bao, Q. Zhang, X. Zhou, *ACS Appl. Energy Mater.* **2023**.
- [30] Z. Wang, J. Hu, Z. Lu, *Batteries Supercaps* **2023**, *6*(4).
- [31] U. Shahzad, H. M. Marwani, M. Saeed, A. M. Asiri, M. R. Repon, R. H. Althomali, M. M. Rahman, *Chem. Rec.* **2024**, *24*(1), e202300285.
- [32] X. X. Luo, X. T. Wang, E. H. Ang, K. Y. Zhang, X. X. Zhao, H. Y. Lu, X. L. Wu, *Chemistry* **2023**, *29*(6), e202202723.
- [33] X. Chen, W. Sun, Y. Wang, *ChemElectroChem* **2020**, *7*(19), 3905–3926.
- [34] Y. Chen, K. Fan, Y. Gao, C. Wang, *Adv. Mater.* **2022**, *34*(52), e2200662.
- [35] B. Dunn, H. Kamath, J.-M. Tarascon, *Science* **2011**, *334*(6058), 928–935.
- [36] P. Simon, Y. Gogotsi, B. Dunn, *Science* **2014**, *343*(6176), 1210–1211.
- [37] M. Zhang, X. Song, X. Ou, Y. Tang, *Energy Storage Mater.* **2019**, *16*, 65–84.
- [38] R. Borah, F. R. Hughson, J. Johnston, T. Nann, *Mater. Today Adv.* **2020**, *6*.
- [39] T. Sun, J. Xie, W. Guo, D. S. Li, Q. Zhang, *Adv. Energy Mater.* **2020**, *10*(19).
- [40] Z. Song, H. Zhou, *Energy Environ. Sci.* **2013**, *6*(8), 2280–2301.
- [41] J. Xie, P. Gu, Q. Zhang, *ACS Energy Lett.* **2017**, *2*(9), 1985–1996.
- [42] H. M. El-Kaderi, J. R. Hunt, J. L. Mendoza-Cortés, A. P. Côté, R. E. Taylor, M. O’Keeffe, O. M. Yaghi, *Science* **2007**, *316*(5822), 268–272.
- [43] F. J. Uribe-Romo, J. R. Hunt, H. Furukawa, C. Klock, M. O’Keeffe, O. M. Yaghi, *J. Am. Chem. Soc.* **2009**, *131*(13), 4570–4571.
- [44] N. Huang, P. Wang, D. Jiang, *Nat. Rev. Mater.* **2016**, *1*(10).
- [45] R. Liu, K. T. Tan, Y. Gong, Y. Chen, Z. Li, S. Xie, T. He, Z. Lu, H. Yang, D. Jiang, *Chem. Soc. Rev.* **2021**, *50*(1), 120–242.
- [46] S. J. Lyle, P. J. Waller, O. M. Yaghi, *Trends Chem.* **2019**, *1*(2), 172–184.
- [47] Y. Li, M. Liu, J. Wu, J. Li, X. Yu, Q. Zhang, *Front. Optoelectron.* **2022**, *15*(1), 38.
- [48] K. Geng, T. He, R. Liu, S. Dalapati, K. T. Tan, Z. Li, S. Tao, Y. Gong, Q. Jiang, D. Jiang, *Chem. Rev.* **2020**, *120*(16), 8814–8933.
- [49] J. Xiao, J. Chen, J. Liu, H. Ihara, H. Qiu, *Green Energy Environ.* **2023**, *8*(6), 1596–1618.
- [50] A. R. Bagheri, N. Aramesh, *J. Mater. Sci.* **2020**, *56*(2), 1116–1132.
- [51] M. J. Bojdys, J. Jeromenok, A. Thomas, M. Antonietti, *Adv. Mater.* **2010**, *22*(19), 2202–5.
- [52] Y. Li, W. Chen, G. Xing, D. Jiang, L. Chen, *Chem. Soc. Rev.* **2020**, *49*(10), 2852–2868.
- [53] X. Li, C. Yang, B. Sun, S. Cai, Z. Chen, Y. Lv, J. Zhang, Y. Liu, J. Mater. Chem. A **2020**, *8*(32), 16045–16060.
- [54] Y. Chen, W. Li, X.-H. Wang, R.-Z. Gao, A.-N. Tang, D.-M. Kong, *Mater. Chem. Front.* **2021**, *5*(3), 1253–1267.
- [55] B. Szczęśniak, S. Borysiuk, J. Choma, M. Jaroniec, *Mater. Horiz.* **2020**, *7*(6), 1457–1473.
- [56] Y. Lu, Y. Cai, Q. Zhang, J. Chen, *J. Phys. Chem. Lett.* **2021**, *12*(33), 8061–8071.
- [57] L. Zhou, S. Jo, M. Park, L. Fang, K. Zhang, Y. Fan, Z. Hao, Y. M. Kang, *Adv. Energy Mater.* **2021**, *11*(27).

- [58] S. Feng, H. Xu, C. Zhang, Y. Chen, J. Zeng, D. Jiang, J. X. Jiang, *Chem. Commun. (Camb.)* **2017**, 53(82), 11334–11337.
- [59] B. Sun, Z. Sun, Y. Yang, X. L. Huang, S. C. Jun, C. Zhao, J. Xue, S. Liu, H. K. Liu, S. X. Dou, *ACS Nano* **2024**, 18(1), 28–66.
- [60] X. Li, Q. Hou, W. Huang, H.-S. Xu, X. Wang, W. Yu, R. Li, K. Zhang, L. Wang, Z. Chen, K. Xie, K. P. Loh, *ACS Energy Lett.* **2020**, 5(11), 3498–3506.
- [61] Z. Li, Z.-W. Liu, Z.-J. Mu, C. Cao, Z. Li, T.-X. Wang, Y. Li, X. Ding, B.-H. Han, W. Feng, *Mater. Chem. Front.* **2020**, 4(4), 1164–1173.
- [62] Y.-N. Gong, X. Guan, H.-L. Jiang, *Coord. Chem. Rev.* **2023**, 475.
- [63] J. Zou, K. Fan, Y. Chen, W. Hu, C. Wang, *Coord. Chem. Rev.* **2022**, 458.
- [64] M. Tang, C. Jiang, S. Liu, X. Li, Y. Chen, Y. Wu, J. Ma, C. Wang, *Energy Storage Mater.* **2020**, 27, 35–42.
- [65] M. Yu, N. Chandrasekhar, R. K. M. Raghupathy, K. H. Ly, H. Zhang, E. Dmitrieva, C. Liang, X. Lu, T. D. Kuhne, H. Mirhosseini, I. M. Weidinger, X. Feng, *J. Am. Chem. Soc.* **2020**, 142(46), 19570–19578.
- [66] D. Ma, H. Zhao, F. Cao, H. Zhao, J. Li, L. Wang, K. Liu, *Chem. Sci.* **2022**, 13(8), 2385–2390.
- [67] L. Zhong, C. Wang, J. He, Z. Lin, X. Yang, R. Li, S. Zhan, L. Zhao, D. Wu, H. Chen, Z. Tang, C. Z. H., H. Lv, *Adv. Mater.* **2024**, e2314050.
- [68] S. Zheng, D. Shi, D. Yan, Q. Wang, T. Sun, T. Ma, L. Li, D. He, Z. Tao, J. Chen, *Angew. Chem. Int. Ed. Engl.* **2022**, 61(12), e202117511.
- [69] H. Peng, S. Huang, V. Montes-Garcia, D. Pakulski, H. Guo, F. Richard, X. Zhuang, P. Samori, A. Ciesielski, *Angew. Chem. Int. Ed. Engl.* **2023**, 62(10), e202216136.
- [70] H. Li, M. Cao, Z. Fu, Q. Ma, L. Zhang, R. Wang, F. Liang, T. Zhou, C. Zhang, *Chem. Sci.* **2024**, 15(12), 4341–4348.
- [71] L. Li, H. Yang, X. Wang, Y. Ma, W. Ou, H. Peng, G. Ma, *J. Mater. Chem. A* **2023**, 11(47), 26221–26229.
- [72] C. Wang, R. Li, Y. Zhu, Y. Wang, Y. Lin, L. Zhong, H. Chen, Z. Tang, H. Li, F. Liu, *Adv. Energy Mater.* **2024**, 14(1), 2302495.
- [73] L. Li, G. Zhang, X. Deng, J. Hao, X. Zhao, H. Li, C. Han, B. Li, *J. Mater. Chem. A* **2022**, 10(39), 20827–20836.
- [74] S. Zhang, Y. L. Zhu, S. Ren, C. Li, X. B. Chen, Z. Li, Y. Han, Z. Shi, S. Feng, *J. Am. Chem. Soc.* **2023**, 145(31), 17309–17320.
- [75] R. Sun, S. Hou, C. Luo, X. Ji, L. Wang, L. Mai, C. Wang, *Nano Lett.* **2020**, 20(5), 3880–3888.
- [76] G. Zou, Z. Tian, V. S. Kale, W. Wang, S. Kandembeth, Z. Cao, J. Guo, J. Czaban-Józwiak, L. Cavallo, O. Shekhah, M. Eddaoudi, H. N. Alshareef, *Adv. Energy Mater.* **2022**, 13(7).
- [77] X. Peng, A. Baktash, Y. Huang, N. Alghamdi, J. You, J. Ning, R. Xin, L. Hao, T. Qiu, B. Wang, L. Zhi, L. Wang, B. Luo, *Energy Storage Mater.* **2024**, 71.
- [78] X. Peng, A. Baktash, N. Alghamdi, M. M. Rana, Y. Huang, X. Hu, C. He, Z. Luo, J. Ning, L. Wang, B. Luo, *Adv. Energy Mater.* **2024**, 14(22).
- [79] H. Lu, F. Ning, R. Jin, C. Teng, Y. Wang, K. Xi, D. Zhou, G. Xue, *ChemSusChem* **2020**, 13(13), 3447–3454.
- [80] J. J. Shea, C. Luo, *ACS Appl. Mater. Interfaces* **2020**, 12(5), 5361–5380.
- [81] T. B. Schon, B. T. McAllister, P. F. Li, D. S. Seferos, *Chem. Soc. Rev.* **2016**, 45(22), 6345–6404.
- [82] C. J. Yao, Z. Wu, J. Xie, F. Yu, W. Guo, Z. J. Xu, D. S. Li, S. Zhang, Q. Zhang, *ChemSusChem* **2020**, 13(9), 2457–2463.
- [83] X. Ma, T. F. Scott, *Commun. Chem.* **2018**, 1(1).
- [84] J. Ming, J. Guo, C. Xia, W. Wang, H. N. Alshareef, *Mater. Sci. Eng.: R: Rep.* **2019**, 135, 58–84.
- [85] P. He, Q. Chen, M. Yan, X. Xu, L. Zhou, L. Mai, C.-W.Nan, *EnergyChem* **2019**, 1(3).
- [86] B. Tang, L. Shan, S. Liang, J. Zhou, *Energy Environ. Sci.* **2019**, 12(11), 3288–3304.
- [87] X. Jia, C. Liu, Z. G. Neale, J. Yang, G. Cao, *Chem. Rev.* **2020**, 120(15), 7795–7866.
- [88] M. Z. Hussein, M. Y. Ghotbi, A. H. Yahaya, M. Z. Abd Rahman, *Mater. Chem. Phys.* **2009**, 113(1), 491–496.
- [89] L. Wang, G. Liu, L. Zou, D. Xue, *J. Alloys Compd.* **2010**, 493(1–2), 471–475.
- [90] G. Ji, J. G. Yao, P. T. Clough, J. C. D. da Costa, E. J. Anthony, P. S. Fennell, W. Wang, M. Zhao, *Energy Environ. Sci.* **2018**, 11(10), 2647–2672.
- [91] R. J. Gummow, G. Vamvounis, M. B. Kannan, Y. He, *Adv. Mater.* **2018**, 30(39), e1801702.
- [92] X. Deng, L. Li, G. Zhang, X. Zhao, J. Hao, C. Han, B. Li, *Energy Storage Mater.* **2022**, 53, 467–481.
- [93] A. Ponrouch, M. R. Palacin, *Curr. Opin. Electrochem.* **2018**, 9, 1–7.
- [94] M. M. Huie, D. C. Bock, E. S. Takeuchi, A. C. Marschilok, K. J. Takeuchi, *Coord. Chem. Rev.* **2015**, 287, 15–27.
- [95] Y. Man, P. Jaumaux, Y. Xu, Y. Fei, X. Mo, G. Wang, X. Zhou, *Sci. Bull. (Beijing)* **2023**, 68(16), 1819–1842.
- [96] Q. Guo, W. Zeng, S.-L. Liu, Y.-Q. Li, J.-Y. Xu, J.-X. Wang, Y. Wang, *Rare Met.* **2020**, 40(2), 290–308.
- [97] F. Ambroz, T. J. Macdonald, T. Nann, *Adv. Energy Mater.* **2017**, 7(15).
- [98] S. K. Das, S. Mahapatra, H. Lahan, *J. Mater. Chem. A* **2017**, 5(14), 6347–6367.
- [99] T. Dutta, J. Mary Gladis, *J. Energy Storage* **2024**, 86.
- [100] Y. Liu, Y. Lu, A. Hossain Khan, G. Wang, Y. Wang, A. Morag, Z. Wang, G. Chen, S. Huang, N. Chandrasekhar, D. Sabagh, D. Li, P. Zhang, D. Ma, E. Brunner, M. Yu, X. Feng, *Angew. Chem. Int. Ed. Engl.* **2023**, 62(30), e202306091.
- [101] P. Zhang, M. Wang, Y. Liu, S. Yang, F. Wang, Y. Li, G. Chen, Z. Li, G. Wang, M. Zhu, R. Dong, M. Yu, O. G. Schmidt, X. Feng, *J. Am. Chem. Soc.* **2021**, 143(27), 10168–10176.
- [102] L. Liu, L. Miao, L. Li, F. Li, Y. Lu, Z. Shang, J. Chen, *J. Phys. Chem. Lett.* **2018**, 9(13), 3573–3579.
- [103] D. Zhu, G. Xu, M. Barnes, Y. Li, C. P. Tseng, Z. Zhang, J. J. Zhang, Y. Zhu, S. Khalil, M. M. Rahman, R. Verduzco, P. M. Ajayan, *Adv. Funct. Mater.* **2021**, 31(32).
- [104] J. Nunes-Pereira, C. M. Costa, S. Lanceros-Méndez, *J. Power Sources* **2015**, 281, 378–398.
- [105] S. Cao, J. Tan, L. Ma, Y. Liu, Q. He, W. Lu, Z. Liu, M. Ye, J. Shen, *Energy Storage Mater.* **2024**, 66.
- [106] Z. Wei, N. Zhang, T. Feng, F. Wu, T. Zhao, R. Chen, *Chem. Eng. J.* **2022**, 430.
- [107] Z. Huang, Y. Chen, Q. Han, M. Su, Y. Liu, S. Wang, H. Wang, *Chem. Eng. J.* **2022**, 429.
- [108] Y. Min, L. Guo, G. Wei, D. Xian, B. Zhang, L. Wang, *Chem. Eng. J.* **2022**, 443, <
- [109] S. Yao, Y. Yang, Z. Liang, J. Chen, J. Ding, F. Li, J. Liu, L. Xi, M. Zhu, J. Liu, *Adv. Funct. Mater.* **2023**, 33(13).
- [110] S. Chen, L. Liang, Y. Li, D. Wang, J. Lu, X. Zhan, Y. Hou, Q. Zhang, J. Lu, *Adv. Energy Mater.* **2023**, 13(11).
- [111] J. Shi, M. Su, H. Li, D. Lai, F. Gao, Q. Lu, *ACS Appl. Mater. Interfaces* **2022**, 14(37), 42018–42029.
- [112] Y. Yang, S. Yao, Z. Liang, Y. Wen, Z. Liu, Y. Wu, J. Liu, M. Zhu, *ACS Energy Lett.* **2022**, 7(2), 885–896.
- [113] C. Yin, Z. Li, D. Zhao, J. Yang, Y. Zhang, Y. Du, Y. Wang, *ACS Nano* **2022**, 16(9), 14178–14187.
- [114] Y. Lu, J. Chen, *Nat. Rev. Chem.* **2020**, 4(3), 127–142.
- [115] C. Luo, G. L. Xu, X. Ji, S. Hou, L. Chen, F. Wang, J. Jiang, Z. Chen, Y. Ren, K. Amine, C. Wang, *Angew. Chem. Int. Ed. Engl.* **2018**, 57(11), 2879–2883.
- [116] C. Luo, O. Borodin, X. Ji, S. Hou, K. J. Gaskell, X. Fan, J. Chen, T. Deng, R. Wang, J. Jiang, C. Wang, *Proc. Natl. Acad. Sci. U. S. A.* **2018**, 115(9), 2004–2009.
- [117] J. Xu, S. An, X. Song, Y. Cao, N. Wang, X. Qiu, Y. Zhang, J. Chen, X. Duan, J. Huang, W. Li, Y. Wang, *Adv. Mater.* **2021**, 33(49), e2105178.
- [118] Y. Peng, G. Xu, Z. Hu, Y. Cheng, C. Chi, D. Yuan, H. Cheng, D. Zhao, *ACS Appl. Mater. Interfaces* **2016**, 8(28), 18505–12.
- [119] K. Jeong, S. Park, G. Y. Jung, S. H. Kim, Y. H. Lee, S. K. Kwak, S. Y. Lee, *J. Am. Chem. Soc.* **2019**, 141(14), 5880–5885.
- [120] Z. Meng, Y. Zhang, M. Dong, Y. Zhang, F. Cui, T.-P. Loh, Y. Jin, W. Zhang, H. Yang, Y. Du, *J. Mater. Chem. A* **2021**, 9(17), 10661–10665.
- [121] S. Kumar, V. V. Kulkarni, R. Jangir, *ChemistrySelect* **2021**, 6(41), 11201–11223.
- [122] R. Guan, L. Zhong, S. Wang, D. Han, M. Xiao, L. Sun, Y. Meng, *ACS Appl. Mater. Interfaces* **2020**, 12(7), 8296–8305.
- [123] Z. Yang, C. Peng, R. Meng, L. Zu, Y. Feng, B. Chen, Y. Mi, C. Zhang, J. Yang, *ACS Cent. Sci.* **2019**, 5(11), 1876–1883.

Manuscript received: August 9, 2024

Revised manuscript received: October 13, 2024

Accepted manuscript online: October 16, 2024

Version of record online: November 13, 2024